

Renormalization Group Theory of the Three-Dimensional Dilute Bose Gas

M. Bijlsma and H.T.C. Stoof

Institute of Theoretical Physics, University of Utrecht, Princetonplein 5

P.O. Box 80.006, 3508 TA Utrecht, The Netherlands

Abstract

We study the three-dimensional atomic Bose gas using renormalization group techniques. Using our knowledge of the microscopic details of the interatomic interaction, we determine the correct initial values of our renormalization group equations and thus obtain also information on nonuniversal properties. As a result, we can predict for instance the critical temperature of the gas and the superfluid and condensate density of the Bose-Einstein condensed phase in the regime $na\Lambda_{th}^2 \ll 1$.

PACS numbers: 03.75.Fi, 05.30.Jp, 32.80.Pj, 64.60.-i

arXiv:cond-mat/9607188v1 26 Jul 1996

Typeset using REVTeX

I. INTRODUCTION

After a long history in which a large number of experimental groups around the world contributed to the development of successful methods to master stabilization and cooling of dilute Bose gases, last year the aim of achieving Bose-Einstein condensation in such a system was finally reached. Indeed, a macroscopic occupation of the one-particle ground state was irrefutably observed in magnetically trapped and evaporatively cooled alkali gas samples of ^{87}Rb and ^{23}Na using relatively simple time-of-flight measurements [1,2]. The transition that was claimed to be seen in an experiment using ^7Li was less convincing [3]. In the latter case, the interatomic interaction is effectively attractive and the potential has a negative scattering length a . Therefore, Bose-Einstein condensation in this system is preempted by a first order phase transition to a liquid or solid phase in the homogeneous case [4]. Nevertheless, for inhomogeneous gas samples the trapping potential has a stabilizing influence and a macroscopic occupation of the ground state is possible in principle. However, when the condensate contains more than some 1500 particles under the conditions of the ^7Li experiment [5], the condensate is still expected to collapse [6].

After these first experiments, which were primarily aimed at proving the existence of a Bose condensate, many experimental groups are now building or improving on their experimental setups to be able to perform much more precise measurements of various interesting properties of the gas in the degenerate regime. Superfluidity [7], the condensate density and its profile, the dynamics of condensate formation [8], the Josephson effect [9], vortex dynamics, collective excitations [10–13] and the precise value of the critical temperature are examples of phenomena and quantities of interest. Other types of experiments will presumably also study the properties of mixtures of atomic gases. In this respect one might think of two bosonic species with a different sign of the scattering length, or mixtures of bosons and fermions, or mixtures uniting both aspects. In the case of a pure fermionic gas of ^6Li atoms, a BCS transition to a superfluid state is predicted to occur and should be within reach of the current experimental technology [14]. Furthermore, in some cases the magnitude and

even the sign of the scattering length can be changed by varying the applied magnetic field. This opens the road to yet another type of experiment.

It is clear from these possibilities that a large number of experiments are expected to be performed in the near future, which clearly makes the degenerate dilute Bose gas also a very interesting subject for theoretical studies. Indeed, this field of research has rapidly expanded during the last year. However, most approaches to the dilute Bose gas use the Bogoliubov (or Popov) theory and are therefore of mean-field type and susceptible to improvements, both from a practical as well as a fundamental point of view. In these approaches one mostly uses the so-called two-body T -matrix, or equivalently the scattering length a . Technically, this important quantity describes the collisions taking place in the dilute Bose gas by summing all possible two-body scattering processes, i.e. all ladder diagrams, without taking into account the fact that the surrounding gaseous medium has an effect on these collisions. However, we have recently shown that the many-body corrections arising from the surrounding gas may be important [15], and are even essential for solving the problem connected to the order of the phase transition which is found to be of first order when using the two-body T -matrix [16–19].

Including quantitatively the same many-body corrections in the case of a highly inhomogeneous gas sample has at this point not yet been done. Moreover, introducing the effect of the medium on two-particle collisions also in the condensed phase by means of the many-body T -matrix leads to fundamental problems if we want to describe the physics at long wavelengths correctly as the ladder diagrams contain infrared divergencies in this case. Using renormalization group techniques, we expect in principle to be capable of resolving these infrared problems as with this method a correct resummation of diagrams is automatically performed, eliminating any potentially troublesome large distance behavior of the individual diagrams. Furthermore, a renormalization group calculation can be used to improve the usual mean-field approaches and the many-body T -matrix theory in the critical region. Indeed, we recently predicted by these means for example that the critical temperature in the ^{87}Rb and ^{23}Na experiments can, due to interaction effects only, be raised with as much

as 10 % compared to the ideal gas value found from the criterion $n_c \Lambda_{th}^3 = \zeta(3/2) \simeq 2.612$ [20], which is identical to the criterion also found using mean-field calculations [15]. Here n is the density and $\Lambda_{th} = (2\pi\hbar^2/mk_B T)^{1/2}$ the thermal de Broglie wavelength of the atoms in the gas. Therefore, it is very well conceivable that in the critical region also other properties of the dilute Bose gas, such as the superfluid and condensate densities, will significantly change when going beyond the mean-field level or beyond the many-body T -matrix theory.

The renormalization group method is a very powerful method which was in first instance developed by Wilson [21] to study the universal properties of second order phase transitions. The basic idea is to perform the trace in the grand canonical partition function $Z_{gr} = Tr(e^{-\beta(\mathcal{H}-\mu\mathcal{N})})$ gradually, starting with the high momentum states. After each step one tries to find a new effective Hamiltonian such that $Z_{gr} = Tr'(e^{-\beta(\mathcal{H}'-\mu'\mathcal{N})})$ and the trace is limited to the low momentum states which have not been reached yet. One proceeds until the complete sum has been performed. Besides the partition function one in this manner also ends up with the effective Hamiltonian describing the long distance properties of the system.

The renormalization group method has been applied to the dilute Bose gas [22–25] before, but without actually performing an extensive quantitative study of this system. This is due to the fact that in general the quantities of nonuniversal nature, such as the critical temperature and the superfluid and condensate densities, depend on the microscopic details of the system considered. Put differently, they depend on the ultraviolet cutoff Λ of the theory and this quantity is usually unknown. However, due to the diluteness of the gas the nonuniversal properties are in the present and forthcoming experiments the most interesting ones, and therefore we are in this paper mainly interested in these aspects. The reason that it is nevertheless possible to perform a quantitative study of the dilute Bose gas using the renormalization group method, is that for this system we do have sufficient information about the microscopic details to calculate and predict the nonuniversal properties. Thus we can, by correctly applying this knowledge, use the renormalization group method and eliminate the cutoff dependence at the same time. We will come back to this point in Sec.

II. Furthermore, we will show that, in contrast to regular perturbation theory, the problems related to the infrared divergencies are in principle indeed resolved, but lead nevertheless to some problems whose solution requires further investigation. However, these problems are only of importance when the interaction energy is no longer negligible compared to the kinetic energy of the particles. The dimensionless parameter reflecting this aspect is $na\Lambda_{th}^2$. Therefore, we will in this paper first concentrate on the regime where $na\Lambda_{th}^2 \ll 1$.

We treat here only the homogeneous Bose gas with effectively repulsive interactions, i.e. with a positive scattering length. However, as in all experiments up till now the number of particles N is so large that the critical temperature T_c is much larger than the energy splitting $\hbar\omega$ between subsequent levels, one can practically for all temperatures use a local density approximation to describe the gas in the trap. The criterion for this description to be valid is that the correlation length should be smaller than the typical length scale on which the atomic density varies. Therefore, a local density approximation breaks down close to the edge of the gas cloud, which is for most practical purposes an unimportant region, but also in the center of the trap if the temperature approaches the critical temperature and the diverging correlation length starts to exceed the typical dimensions of the trap. The temperature interval where this occurs has a width of $O(T_c(\hbar\omega/k_B T_c))$ around the critical temperature. As this region is very small, we conclude that the results we find in this paper for the homogeneous gas are essentially also valid for the inner part of the trapped Bose gases, and in particular pertain to the ^{87}Rb and ^{23}Na experiments. Furthermore, we want to remark here that it would in principle also be possible to set up a renormalization group calculation for the inhomogeneous Bose gas. Of course, there is no real second order phase transition present in this system because the correlation length ξ can never become infinite, but the techniques of renormalization group as presented in this article can still be used to calculate the (nonuniversal) properties also in this case.

The paper is organized as follows. In Sec. II we briefly discuss the theoretical description of the dilute Bose gas and the renormalization group method. In Sec. III we first apply the renormalization group to the uncondensed phase of the Bose gas because the flow equations

are relatively simple and easy to understand in this case. In Sec. IV we then go over to the degenerate Bose gas and again describe the gas properties following from the renormalization group approach. Finally, in Sec. V we end with some concluding remarks. In the numerical calculations we always use ^{23}Na as an example, because the experiment with this atomic species is closest to the conditions of homogeneity [2]. We take in these cases the most up-to-date value of $52a_0$ for the two-body scattering length [26].

II. THE RENORMALIZATION GROUP

The renormalization group equations are most easily obtained using the functional integral formulation of the grand canonical partition function [27]. We thus write

$$Z_{gr} = \text{Tr}(e^{-\beta(\mathcal{H}-\mu N)}) = \int d[\psi^*]d[\psi] \exp \left\{ -\frac{1}{\hbar} S[\psi^*, \psi] \right\} . \quad (1)$$

This functional integral is over c -number fields $\psi^*(\mathbf{x}, \tau)$ and $\psi(\mathbf{x}, \tau)$ periodic in imaginary time over $\hbar\beta = \hbar/k_B T$. The so-called Euclidian action for the dilute Bose gas is given by

$$S[\psi^*, \psi] = \int_0^{\hbar\beta} d\tau \left(\int d\mathbf{x} \psi^*(\mathbf{x}, \tau) \left[\hbar \frac{\partial}{\partial \tau} - \frac{\hbar^2 \nabla^2}{2m} - \mu \right] \psi(\mathbf{x}, \tau) + \frac{1}{2} \int d\mathbf{x} \int d\mathbf{x}' \psi^*(\mathbf{x}, \tau) \psi^*(\mathbf{x}', \tau) V(\mathbf{x} - \mathbf{x}') \psi(\mathbf{x}', \tau) \psi(\mathbf{x}, \tau) \right) , \quad (2)$$

with μ the chemical potential and $V(\mathbf{x} - \mathbf{x}')$ the effectively repulsive interaction potential. In principle, the action also contains a term describing three-particle interactions, i.e.

$$\frac{1}{6} \int_0^{\hbar\beta} d\tau \int d\mathbf{x} \int d\mathbf{x}' \int d\mathbf{x}'' \psi^*(\mathbf{x}, \tau) \psi^*(\mathbf{x}', \tau) \psi^*(\mathbf{x}'', \tau) U(\mathbf{x} - \mathbf{x}', \mathbf{x} - \mathbf{x}'') \psi(\mathbf{x}'', \tau) \psi(\mathbf{x}', \tau) \psi(\mathbf{x}, \tau) ,$$

and terms describing interactions between four and more particles due to the finite extent of the electron clouds of the atoms. However, as we are describing the *dilute* Bose gas these terms are expected to make in general no significant contribution to the thermodynamic properties to be calculated. Indeed, in usual approaches to the dilute Bose gas these terms are always neglected for this very reason. One aspect of the renormalization group calculation is that it is possible, and even rather straightforward, to include the three-body

interaction in the calculations. As its influence will turn out to be extremely small, except in the critical region where it becomes somewhat larger, we will in the rest of this section omit this term for reasons of brevity. However, in Sec. III we perform some calculations including the three-body term to show its effect quantitatively, and at that point introduce it again.

Expanding the fields in Fourier modes through

$$\psi(\mathbf{x}, \tau) = \frac{1}{(\hbar\beta V)^{1/2}} \sum_{\mathbf{k}, n} a_{\mathbf{k}, n} e^{i(\mathbf{k}\cdot\mathbf{x} - \omega_n \tau)} \quad (3)$$

and the complex conjugate expression for $\psi^*(\mathbf{x}, \tau)$, we can write the action in momentum space as

$$S[a^*, a] = \sum_{\mathbf{k}, n} (-i\hbar\omega_n + \epsilon_{\mathbf{k}} - \mu) a_{\mathbf{k}, n}^* a_{\mathbf{k}, n} + \frac{1}{2} \frac{1}{\hbar\beta V} \sum_{\substack{\mathbf{k}, \mathbf{k}', \mathbf{q} \\ n, n', m}} V_{\mathbf{q}} a_{\mathbf{k}+\mathbf{q}, n+m}^* a_{\mathbf{k}'-\mathbf{q}, n'-m}^* a_{\mathbf{k}', n'} a_{\mathbf{k}, n} . \quad (4)$$

In this equation $\epsilon_{\mathbf{k}} = \hbar^2 \mathbf{k}^2 / 2m$ is the kinetic energy, $V_{\mathbf{q}} = \int d\mathbf{x} V(\mathbf{x}) e^{-i\mathbf{q}\cdot\mathbf{x}}$ is the Fourier transform of the interaction potential, V is volume of the system and the bosonic Matsubara frequencies $\omega_n = 2\pi n / \hbar\beta$ reflect the periodicity of the fields in imaginary time.

The renormalization group equations now follow from repeatedly applying the renormalization group transformation to this action. It consists of three different stages [21,28] which we summarize here. The first step is to perform the functional integral in Eq. (1) for the most rapidly oscillating fields. In other words, we eliminate the highest Fourier modes from the action in Eq. (4). In practice, we therefore have to split the fields in ‘slow modes’ and ‘fast modes’, i.e. we define

$$\begin{aligned} \psi_{<}(\mathbf{x}, \tau) &= \frac{1}{(\hbar\beta V)^{1/2}} \sum_{\mathbf{k}, n} a_{\mathbf{k}, n} e^{i(\mathbf{k}\cdot\mathbf{x} - \omega_n \tau)} \quad \text{for } 0 < |\mathbf{k}| < \Lambda - d\Lambda \\ \psi_{>}(\mathbf{x}, \tau) &= \frac{1}{(\hbar\beta V)^{1/2}} \sum_{\mathbf{k}, n} a_{\mathbf{k}, n} e^{i(\mathbf{k}\cdot\mathbf{x} - \omega_n \tau)} \quad \text{for } \Lambda - d\Lambda < |\mathbf{k}| < \Lambda \end{aligned} \quad (5)$$

where Λ is the ultraviolet cutoff in the theory, and $d\Lambda$ is the thickness of the shell in momentum space which is going to be integrated out. We will dwell on the issue of the ultraviolet cutoff shortly. With the definitions in Eq. (5), we can write the action as

$$S[\psi^*, \psi] = S_0[\psi_{<}^*, \psi_{<}] + S_0[\psi_{>}^*, \psi_{>}] + S_I[\psi_{<}^*, \psi_{<}, \psi_{>}^*, \psi_{>}], \quad (6)$$

where S_0 is quadratic in the fields, and S_I contains the remaining terms, and in particular the terms that couple the slow and fast modes. The partition function can now be written as

$$\begin{aligned} Z_{gr} &= \int d[\psi_{<}^*]d[\psi_{<}] \exp \left\{ -\frac{1}{\hbar} S_0[\psi_{<}^*, \psi_{<}] \right\} \times \int d[\psi_{>}^*]d[\psi_{>}] \exp \left\{ -\frac{1}{\hbar} (S_0[\psi_{>}^*, \psi_{>}] + S_I[\psi_{<}^*, \psi_{<}, \psi_{>}^*, \psi_{>}]) \right\} \\ &\equiv \int d[\psi_{<}^*]d[\psi_{<}] \exp \left\{ -\frac{1}{\hbar} S_0[\psi_{<}^*, \psi_{<}] \right\} \times \exp \left\{ -\frac{1}{\hbar} \Delta S[\psi_{<}^*, \psi_{<}] \right\} . \end{aligned} \quad (7)$$

After performing the last integral, we obtain an expression for the partition function containing the new effective action $S'[\psi_{<}^*, \psi_{<}] = S_0[\psi_{<}^*, \psi_{<}] + \Delta S[\psi_{<}^*, \psi_{<}]$ for the slow modes. The effect of this mode elimination is to change the value of the existing coupling constants and to introduce new vertices in the original action. The discussion of the rules on how we can obtain the equations describing this change of the coupling constants in general will be deferred to Secs. III and IV where we will also apply these rules to find the flow equations for the Bose system. The two remaining stages of the renormalization group transformation consist of a rescaling of the momenta such that the new cutoff, which is $\Lambda - d\Lambda$, is restored to its initial value Λ , and a rescaling of the frequency and fields in the action such that there is no effect from this momentum rescaling on some appropriate terms in the quadratic part of the action. If we neglect the renormalizations from the first step, this procedure yields the so-called trivial scaling of the coupling constants and reveals the relevance of the various vertices as it tells whether the value of the corresponding coupling constant grows (termed relevant), remains the same (termed marginal), or shrinks (termed irrelevant) as we scale the ultraviolet cutoff. Having completed these final steps of the renormalization group transformation, we can read off the new coupling constants from the action. Thus, the renormalization group equations have two contributions. One is from the rescaling, the other is from the actual integrating out of high momenta from the action.

Concerning the trivial scaling, there are two cases to distinguish. For the normal renormalization group equations this scaling is found using the full quadratic action. The other situation occurs exactly at the critical temperature. At that point the correlation length ξ of the system is infinite, and the system looks the same on every length scale. Hence, the cou-

pling constants remain the same when performing the renormalization group transformation and we are at a fixed point. To find this fixed point from the set of renormalization group equations, we generally have to use a different scaling from the one found above, and this is the scaling at the critical temperature. It can easily be obtained by realizing that the correlation time τ_c also diverges as we approach the critical temperature, behaving like $\tau_c \propto \xi^z$. At temperatures such that $\hbar\beta \ll \tau_c$, we can neglect the time dependence in the action and the $\partial/\partial\tau$ -term in the quadratic part of the action is unimportant. As a result, we then only need to consider the kinetic energy term to find the trivial scalings. This yields the scaling at the critical temperature. In renormalization group studies, one normally restricts oneself to couplings which are relevant or marginal at the critical temperature, and this we will in first instance also do. However, it turns out that even the marginal coupling constant U_0 from the three-body interaction term is quite irrelevant to the nonuniversal properties to be calculated. This is of course due to the fact that three-body interactions are unimportant for a *dilute* system. However, if one is interested in the universal properties of the phase transition, such as e.g. the critical exponent ν connected to the divergence of the correlation length when approaching the critical temperature, marginal and also irrelevant couplings can have a considerable effect. We will explicitly encounter this fact in the next section. Also the position of the fixed point is changed when including irrelevant couplings.

The renormalization group equations describe the change of the coupling constants as we integrate out momentum shells from the action. Having arrived at the long wavelength effective action, we find whether or not we are in the condensed phase, and we can calculate universal properties connected to this phase transition. However, our aim is to use the renormalization group method to obtain information on other properties as well. In particular, we want to calculate the equation of state, the superfluid density, and the pressure of the gas. This can also straightforwardly be done by noting that e.g. for the total density we have $n = \sum_{\mathbf{k},n} \langle a_{\mathbf{k},n}^* a_{\mathbf{k},n} \rangle$. This equation can be cast into a differential equation describing the building up of the density as we proceed with the elimination of the fast Fourier modes. For that purpose, we have to use the right value of the chemical potential μ in each subsequent

momentum shell as found from the renormalization group equations. In the same fashion one can also determine e.g. the superfluid density and the thermodynamic potential.

Before we can start with the derivation of the flow equations, we first have to pay some attention to the high momentum limit of the action. In principle, there is no real sharp ultraviolet cutoff Λ in our problem. However, the typical behavior of the Fourier transform of the two-body interaction potential, depicted in Fig. 1, is such that there is an effective ultraviolet cutoff around the momentum scale set by the scattering length a of this potential. Below this value, the Fourier transform is practically momentum independent and equal to V_0 . As in the Bose systems considered here and realized experimentally the temperatures are so low that $\hbar/a \gg \hbar/\Lambda_{th}$, the particles in the gas reside in a momentum range well below this ultraviolet cutoff. Thus, we can represent the interaction potential by the momentum independent value V_0 for momenta below a cutoff $\hbar\Lambda$ of $O(\hbar/a)$, and zero for larger momenta.

Modelling the potential as such implies that the nonuniversal properties we find from a renormalization group calculation will be sensitive to the specific value of the cutoff Λ taken in the calculations. However, at this point our knowledge about the microscopic details of the Bose gas comes in to resolve this potential problem. In particular, we know that the two-body interaction potential $V_{\mathbf{q}}$ has to renormalize to the two-body T -matrix $T^{2B}((\mathbf{k} - \mathbf{k}')/2 + \mathbf{q}, (\mathbf{k} - \mathbf{k}')/2; \hbar^2(\mathbf{k} - \mathbf{k}')^2/m)$ when we include all possible two-body scattering processes in the vacuum [29]. The two-body T -matrix roughly has the same momentum dependence as $V_{\mathbf{q}}$, cf. Fig. 1, and is in particular constant and equal to $4\pi a\hbar^2/m$ in the range of thermal momenta and energies. Thus, given an ultraviolet cutoff Λ we can fix the renormalization group equations by demanding that for the two-body problem, V_0 indeed correctly renormalizes to $4\pi a\hbar^2/m$. Since this value is, due to the inequality $a/\Lambda_{th} \ll 1$, already attained before we enter the thermal regime as we integrate out more and more momentum shells from the action, this indeed leads to a correct description of the properties of the Bose gas which is independent of the ultraviolet cutoff Λ . Having eliminated the cutoff dependence, we are then in a position to determine also the nonuniversal properties of the dilute Bose gas. Furthermore, we can perform the calculation for any (positive) value of the

scattering length, thus being able to describe any atomic species with effectively repulsive s -wave scattering. The results we find are therefore relevant to the current experiments using ^{87}Rb and ^{23}Na , but also to future experiments using atomic hydrogen or other atoms with a positive scattering length.

We now turn to the application of the renormalization group method to the dilute Bose gas. First, we derive the renormalization group equations when the chemical potential is negative, starting from the action in Eq. (4). These equations however, do not describe the Bose condensed phase for then it is required that the chemical potential be positive. As a result, we have to rederive the renormalization group equations for that case and this is carried out in Sec. IV. The derivation is now much more involved as the space and time independent part of the effective action, i.e. $-\mu |a_{\mathbf{0},0}|^2 + V_{\mathbf{0}} |a_{\mathbf{0},0}|^4 / 2\hbar\beta V$, has for $\mu > 0$ a Mexican hat shape and we first have to expand the action around the correct extremum by performing the shift $a_{\mathbf{0},0} \rightarrow a_{\mathbf{0},0} + \sqrt{n_{\mathbf{0}}\hbar\beta V}$ and introducing the condensate density $n_{\mathbf{0}}$. Only after that can we proceed to find the contributions to the renormalization of the vertices.

III. THE SYMMETRY UNBROKEN PHASE

In this section we first concentrate on the renormalization group equations valid for negative chemical potential. The reasons for this are threefold. The equations correctly describe the Bose gas in the uncondensed phase, and they offer an easy way to determine the influence of three-body effects on the quantities of interest. Moreover, it is best to start with this relatively simple set of equations because it illuminates most clearly our procedure to eliminate the cutoff dependence of the theory.

A. The flow equations

To calculate the change of the couplings after each step of the renormalization group transformation we can technically proceed in two different, but equivalent ways. The first and probably most familiar method is to expand the integrand in the partition function in

powers of $S_I[\psi_{<}^*, \psi_{<}, \psi_{>}^*, \psi_{>}]$, and then perform the integrals over the fast modes by evaluating the appropriate Feynman diagrams contributing to the renormalization or flow of the vertices of interest. The renormalization of the gradient and time-derivative terms of interest are found by performing a Taylor expansion in external momenta and frequencies of these diagrams. However, the associated couplings become more and more irrelevant for higher order terms in this expansion. The integration over the internal momenta of the diagrams is restricted to the afore-mentioned momentum shell, which can in principle be chosen to have any thickness $d\Lambda$. Taking it infinitesimally small, possible in the thermodynamic limit only, leads to a continuous renormalization group transformation described by a coupled set of first order differential equations. A much more important reason to take $d\Lambda$ infinitesimal is that in this case the type of diagrams which contribute to the renormalization are the so-called one-loop diagrams only. This is a point which is not always explicit in the literature, but it follows from the fact that each extra loop, i.e. each extra momentum integral, introduces an extra factor of $d\Lambda$ [30], and therefore will vanish when $d\Lambda$ is infinitesimal. Clearly, this is not so when the thickness $d\Lambda$ has a finite value. Note furthermore that the above holds irrespective of the magnitude of the interactions, in contrast to what is sometimes mentioned in the literature [22,24]. In the case of e.g. a large two-body interaction vertex, the infinitesimal thickness of the momentum shell still ascertains the validity of a perturbation expansion with the use of one-loop diagrams only. This most notably implies that in this formulation the restrictions of the renormalization group method lie in the number of vertices considered, and not in the type of diagrams taken into account. The second way to obtain the renormalization group equations does not explicitly make use of Feynman diagrams, and is therefore very useful and efficient when the number of diagrams is large and/or the associated combinatorics is complicated. We here use the diagrammatic method as in the unbroken phase the number of diagrams is limited and the combinatorics is simple. We use the other method in Sec. IV. Moreover, using Feynman graphs also gives a transparent way to find the trivial scaling of the vertices in a somewhat different fashion than from the rescaling procedure described in Sec. II, which brings out more clearly the

physics of this procedure.

As mentioned before, we include in first instance also the three-body interaction term written down in the previous section into our considerations, and take it, as the two-body interaction, to be momentum independent below the cutoff Λ . The one-loop diagrams to be calculated are depicted in Fig. 2. We find that in the thermodynamic limit the total contribution to the chemical potential from integrating out an infinitesimal momentum shell in the Hartree and Fock diagrams is

$$d\mu = -2V_0 \int_{\Lambda(l)-d\Lambda}^{\Lambda(l)} \frac{d^3\mathbf{k}}{(2\pi)^3} N(\epsilon_{\mathbf{k}} - \mu) , \quad (8)$$

where $\Lambda(l) = \Lambda e^{-l}$ denotes the radius of the shell in momentum space. The ladder and bubble diagrams renormalizing the two-body interaction potential give, together with the diagram containing the three-body term,

$$dV_0 = -V_0^2 \int_{\Lambda(l)-d\Lambda}^{\Lambda(l)} \frac{d^3\mathbf{k}}{(2\pi)^3} \frac{1 + 2N(\epsilon_{\mathbf{k}} - \mu)}{2(\epsilon_{\mathbf{k}} - \mu)} - 4V_0^2 \int_{\Lambda(l)-d\Lambda}^{\Lambda(l)} \frac{d^3\mathbf{k}}{(2\pi)^3} \beta N(\epsilon_{\mathbf{k}} - \mu) [N(\epsilon_{\mathbf{k}} - \mu) + 1] +$$

$$3U_0 \int_{\Lambda(l)-d\Lambda}^{\Lambda(l)} \frac{d^3\mathbf{k}}{(2\pi)^3} N(\epsilon_{\mathbf{k}} - \mu) , \quad (9)$$

and for the vertex U_0 we find

$$dU_0 = 8V_0^3 \int_{\Lambda(l)-d\Lambda}^{\Lambda(l)} \frac{d^3\mathbf{k}}{(2\pi)^3} \beta^2 N(\epsilon_{\mathbf{k}} - \mu) [N(\epsilon_{\mathbf{k}} - \mu) + 1] [2N(\epsilon_{\mathbf{k}} - \mu) + 1] +$$

$$3V_0^3 \int_{\Lambda(l)-d\Lambda}^{\Lambda(l)} \frac{d^3\mathbf{k}}{(2\pi)^3} \frac{1}{(\epsilon_{\mathbf{k}} - \mu)^2} [1 + 2N(\epsilon_{\mathbf{k}} - \mu) + 2\beta(\epsilon_{\mathbf{k}} - \mu)N(\epsilon_{\mathbf{k}} - \mu) [N(\epsilon_{\mathbf{k}} - \mu) + 1]] -$$

$$U_0 V_0 \int_{\Lambda(l)-d\Lambda}^{\Lambda(l)} \frac{d^3\mathbf{k}}{(2\pi)^3} \left[\frac{3(1 + 2N(\epsilon_{\mathbf{k}} - \mu))}{\epsilon_{\mathbf{k}} - \mu} + 18\beta N(\epsilon_{\mathbf{k}} - \mu) [N(\epsilon_{\mathbf{k}} - \mu) + 1] \right] . \quad (10)$$

In these expressions $N(\epsilon_{\mathbf{k}} - \mu) = 1/(e^{\beta(\epsilon_{\mathbf{k}} - \mu)} - 1)$ is the Bose-Einstein distribution function which result from the summation over the Matsubara frequencies ω_n .

To derive the renormalization group equations and the trivial scalings of the coupling constants we focus on the first of these equations renormalizing the chemical potential, and

cast it into a differential equation. Using $|\mathbf{k}| = \Lambda(l) = \Lambda e^{-l}$ and performing the angular integrals, we can write Eq. (8) as

$$d\mu = -2V_0 \frac{\Lambda^3}{2\pi^2} \int_l^{l+dl} N(\epsilon_\Lambda e^{-2l} - \mu) e^{-3l} dl . \quad (11)$$

Next, we remove all explicit l -dependencies from the Bose-Einstein distribution function by letting both the temperature and the chemical potential scale with exponent 2, i.e. we put $T(l) = T e^{2l}$ and $\mu(l) = \mu e^{2l}$. Hence, both temperature and chemical potential scale trivially with exponent 2 and we find for the differential equation describing the change of the chemical potential when integrating out a momentum shell

$$\frac{d\mu}{dl} = 2\mu - \frac{\Lambda^3}{\pi^2} V_0 e^{-l} N(\epsilon_\Lambda - \mu) . \quad (12)$$

Finally, we now also absorb the factor e^{-l} into V_0 in order to remove the remaining explicit l -dependence. As a result, V_0 scales trivially with exponent -1 . By considering in Eq. (9) the term containing U_0 , we can analogously show that this vertex trivially scales with an exponent -4 . Note that to find the real physical quantities we should always remove the trivial scalings again. We see that the trivial scaling can, in a very simple way, be found from the one-loop expressions. Moreover, it shows that introducing the trivial scalings does not have an essential effect on the renormalization of the vertices; it is merely a rewriting of the differential equations. In the case of a negative chemical potential we eventually obtain the following coupled set of renormalization group equations for the coupling constants μ , V_0 and U_0 ,

$$\frac{d\mu}{dl} = 2\mu - \frac{\Lambda^3}{\pi^2} V_0 N(\epsilon_\Lambda - \mu) , \quad (13a)$$

$$\begin{aligned} \frac{dV_0}{dl} = & -V_0 - \frac{\Lambda^3}{2\pi^2} V_0^2 \left[\frac{1 + 2N(\epsilon_\Lambda - \mu)}{2(\epsilon_\Lambda - \mu)} + 4\beta N(\epsilon_\Lambda - \mu)[N(\epsilon_\Lambda - \mu) + 1] \right] \\ & + \frac{3\Lambda^3}{2\pi^2} U_0 N(\epsilon_\Lambda - \mu) , \end{aligned} \quad (13b)$$

$$\frac{dU_0}{dl} = -4U_0 + \frac{\Lambda^3}{2\pi^2} V_0^3 \left[8\beta^2 N(\epsilon_\Lambda - \mu)[N(\epsilon_\Lambda - \mu) + 1][2N(\epsilon_\Lambda - \mu) + 1] + \right.$$

$$\frac{3}{(\epsilon_\Lambda - \mu)^2} [1 + 2N(\epsilon_\Lambda - \mu) + 2\beta(\epsilon_\Lambda - \mu)N(\epsilon_\Lambda - \mu)[N(\epsilon_\Lambda - \mu) + 1]] - \frac{\Lambda^3}{2\pi^2} U_0 V_0 \left[\frac{3(1 + 2N(\epsilon_\Lambda - \mu))}{\epsilon_\Lambda - \mu} + 18\beta N(\epsilon_\Lambda - \mu)[N(\epsilon_\Lambda - \mu) + 1] \right]. \quad (13c)$$

To argue that these equations are the only ones we need to consider, we still have to determine the trivial scaling at the critical temperature. This different scaling comes about because in the limit $l \rightarrow \infty$ the Bose-Einstein distribution function behaves as $N(\epsilon_\Lambda - \mu) = 1/\beta(l)(\epsilon_\Lambda - \mu(l))$ as we are effectively at very high temperatures due to $\beta(l) = \beta e^{-2l}$. To remove again all explicit l -dependencies after substituting this behavior, we clearly need a different trivial scaling of the vertices, and this is precisely the trivial scaling at the critical temperature, since putting $N(\epsilon_\Lambda - \mu) = 1/\beta(\epsilon_\Lambda - \mu)$ is equivalent to neglecting the time-derivative in the action. In this manner we can straightforwardly show that the scaling of the chemical potential remains the same, i.e. we have $\mu(l) = \mu e^{2l}$, that the scaling of the two-body interaction becomes $V_0(l) = V_0 e^l$ instead of $V_0(l) = V_0 e^{-l}$, and that the three-body interaction does not scale, i.e. $U_0(l) = U_0$ instead of $U_0(l) = U_0 e^{-4l}$. From this we conclude that μ and V_0 are relevant and U_0 is marginal at the critical temperature. Furthermore, the four-body interaction is indeed irrelevant and therefore not included in the calculations. The coefficients of the gradient and time derivative terms in the quadratic part of the action are, like U_0 , marginal and would in principle also have to be included in the renormalization group equations. However, as we are in the regime $a/\Lambda_{th} \ll 1$, the interactions are expected to be independent of momentum and energy (but see below) and there is no renormalization of the $\partial/\partial\tau$ and $|\nabla|^2$ terms. Moreover, we know from the ϵ -expansion that the anomalous dimension η , indicating the importance of the $|\nabla|^2$ renormalization at the critical temperature, is very small, namely $\eta = 0.02$ [31]. Therefore, the $\partial/\partial\tau$ and $|\nabla|^2$ renormalizations will be neglected and Eq. (13) describes the renormalization of the vertices we will consider.

To calculate the partition function of the gas, we need, next to the flow equations for the above quantities, also the correct boundary conditions. The first one for the chemical potential μ is just the bare value in the action Eq. (4). For the two-body interaction potential

$V_{\mathbf{0}}$ we need to be more careful, as this vertex has to correctly fix the renormalization group equations as described in the previous section. From Eq. (13b) we recognize that in a vacuum, i.e. $N(\epsilon_{\Lambda} - \mu) = 0$, the renormalization of the interaction between two particles is governed by

$$\frac{dV_{\mathbf{0}}}{dl} = -V_{\mathbf{0}} - \frac{\Lambda^3}{2\pi^2} V_{\mathbf{0}}^2 \frac{1}{2(\epsilon_{\Lambda} - \mu)}. \quad (14)$$

This is just the differential form of the Lippmann-Schwinger equation [29] for the two-body T -matrix at energy 2μ , i.e. $T^{2B}(\mathbf{0}, \mathbf{0}; 2\mu)$. As the two-body T -matrix is energy independent for low energies, we can neglect μ and use $T^{2B}(\mathbf{0}, \mathbf{0}; 2\mu) \simeq T^{2B}(\mathbf{0}, \mathbf{0}; 0) = 4\pi a \hbar^2/m$. As the solution of Eq. (14) is also practically independent of the chemical potential, we can there also neglect it. As a result, the requirement is now that, given an ultraviolet cutoff Λ , $V_{\mathbf{0}}$ flows for $l \rightarrow \infty$ to the value $4\pi a \hbar^2/m$. This can be ascertained by choosing the right initial condition for $V_{\mathbf{0}}$, and more precisely we find from analytically solving Eq. (14) that

$$V_{\mathbf{0}}(l = 0) = \frac{4\pi a \hbar^2}{m} \frac{1}{1 - 2a\Lambda/\pi} \quad (15)$$

leads to the correct result. Note that we can describe different atomic species by only changing the value of the scattering length a used in this equation. Finally, we in principle also need a boundary condition for the three-body interaction $U_{\mathbf{0}}$. For this interaction we can, analogous to the scattering length a for the two-body interaction, introduce a length scale b , and again fix $U_{\mathbf{0}}(l = 0)$ such that the renormalization group calculation gives the correct result $U_{\mathbf{0}}(l = \infty) = 4\pi \hbar^2 b^4/m$ for elastic three-body scattering in a vacuum. However, in general not much is known about the microscopic details of the three-body interaction in a dilute Bose gas, and in particular about the value of the ‘three-body scattering length’ b . But, as can be expected from the fact that the three-body interactions are in the renormalization group sense irrelevant at large momenta, the results are practically insensitive to the boundary value of $U_{\mathbf{0}}$ used, and $U_{\mathbf{0}}(l = 0)$ is hardly of any importance. This is shown explicitly in Sec. IIIB where we analyze the results from the renormalization group approach for ^{23}Na . Note, that taking $U_{\mathbf{0}}(l = 0) = 0$ is equivalent to assuming that three-particle

scattering is solely due to the sum of pair interactions. This is a standard approximation in atomic three-body calculations.

Finally, to describe the dilute Bose gas we still need to derive expressions for the total and superfluid density, and the equation giving the thermodynamic potential Ω , and thus the pressure $p = -\Omega/V \equiv -\omega$. To do so, we make use of the following well-known one-loop expressions for the density

$$n = \int_0^\Lambda \frac{d^3\mathbf{k}}{(2\pi)^3} N(\epsilon_{\mathbf{k}} - \mu) , \quad (16)$$

the superfluid density

$$n_s = n - n_n = n - \int_0^\Lambda \frac{d^3\mathbf{k}}{(2\pi)^3} \frac{2}{3} \beta \epsilon_{\mathbf{k}} N(\epsilon_{\mathbf{k}} - \mu) [N(\epsilon_{\mathbf{k}} - \mu) + 1] , \quad (17)$$

where n_n is the normal density given by the momentum-momentum correlation function, and the thermodynamic potential

$$\omega = \frac{1}{\beta} \int_0^\Lambda \frac{d^3\mathbf{k}}{(2\pi)^3} \ln(1 - e^{-\beta(\epsilon_{\mathbf{k}} - \mu)}) . \quad (18)$$

Casting these equations into a differential form by performing the integration shell by shell leads to

$$\frac{dn}{dl} = \frac{\Lambda^3}{2\pi^2} N(\epsilon_\Lambda - \mu) e^{-3l} \quad (19a)$$

$$\frac{dn_s}{dl} = \frac{dn}{dl} - \frac{\Lambda^3}{3\pi^2} \beta \epsilon_\Lambda N(\epsilon_\Lambda - \mu) [N(\epsilon_\Lambda - \mu) + 1] e^{-3l} \quad (19b)$$

$$\frac{d\omega}{dl} = \frac{1}{\beta} \frac{\Lambda^3}{2\pi^2} \ln(1 - e^{-\beta(\epsilon_\Lambda - \mu)}) e^{-5l} , \quad (19c)$$

where the inverse temperature again scales as $\beta(l) = \beta e^{-2l}$ and the chemical potential is found from Eq. (13a) at each step of the integration. These equations describe the building up of these quantities as we integrate out more and more momentum shells from the action. For convenience, the explicit l -dependence is not removed from these equations, and they thus immediately yield the physical quantities. Note furthermore that these equations have no influence on the renormalization of μ , V_0 , and U_0 as they are decoupled from the renormalization group equations (13).

B. Analysis of the flow equations

We start our analysis by first focussing on the critical properties of Eq. (13) and in particular on the critical exponent ν pertaining to the divergence of the correlation length, i.e. the correlation length behaves as $\xi = \xi_0 |(T - T_c)/T_c|^{-\nu}$ when approaching the critical temperature. For that purpose we have to find the fixed point of the renormalization group equations, linearize the flow equations around this fixed point and identify the largest eigenvalue λ_+ which is related to this critical exponent via $\nu = 1/\lambda_+$ [21]. We in first instance omit the three-body interaction, but in a subsequent calculation include it again to determine the influence of this marginal vertex on the value of ν . Only for the set $\{\mu, V_0\}$, when $U_0(l) = 0$, do we perform the calculation of the fixed point explicitly. With the remarks made in Sec. IIIA we have that the fixed point is found from

$$\frac{d\mu}{dl} = 2\mu - \frac{\Lambda^3}{\pi^2} V_0 \frac{k_B T}{\epsilon_\Lambda - \mu} = 0 \quad (20a)$$

$$\frac{dV_0}{dl} = V_0 - \frac{\Lambda^3}{2\pi^2} V_0^2 \frac{5k_B T}{(\epsilon_\Lambda - \mu)^2} = 0 \quad (20b)$$

yielding $(\mu^*, V_0^*) = (\epsilon_\Lambda/6, 5\pi^2\epsilon_\Lambda^2/18k_B T\Lambda^3)$. From linearization of the Eqs. (20a) and (20b) around this value we find for the largest eigenvalue $\lambda_+ = 1.878$, implying that $\nu = 0.532$. Repeating the calculation including the equation for $U_0(l)$, the fixed point is shifted and the critical exponent is found to be $\nu = 0.613$. Thus, we see that the marginal operator U_0 has a rather large effect. Moreover, we can conclude from this result that also irrelevant coupling constants must have a considerable effect as it is known, from the ϵ -expansion of the $O(2)$ -model [31] and from measurements in ^4He experiments, that the true critical exponent of the Bose gas should have the value $\nu = 0.67$. This discrepancy should be alleviated by including more and more irrelevant vertices.

However, as we are in particular interested in the nonuniversal properties of the dilute Bose gas, we now turn to the influence of the three-body interaction term U_0 on these quantities. The influence of this term will of course be largest when we start close to

the critical chemical potential, because at the critical point in principle all fluctuations are of importance. Starting with a chemical potential near the critical value leads to a trajectory that almost flows into the fixed point of the renormalization group equations, and the momentum interval in which irrelevant vertices can have a significant contribution to the flow, and also to the building up of the density, is then largest. The bare chemical potential yielding a flow into the fixed point is positive, and the physical chemical potential (i.e. with the trivial scaling removed) renormalizes to zero. For a bare chemical potential larger than this critical value the flow is no longer defined as at some value of l we have that $(\epsilon_\Lambda - \mu(l))$ becomes zero and the Bose-Einstein distribution function diverges. We will come back to this point later on and restrict ourselves here to the accessible regime, which physically implies that $n < n_c$.

The first aspect connected to the three-body interaction concerns the initial value problem for U_0 . Indeed, as alluded to before, an explicit calculation shows that changing the boundary condition for U_0 from 0 to one corresponding with a ‘three-body scattering length’ $b = 10a = 520a_0$, which is extremely large in general, changes the total density and the pressure in the system with less than 0.1 %. Thus, the results we obtain are practically insensitive to this boundary condition and henceforth we simply use $b = a = 52a_0$. The second aspect we want to consider is the influence of the three-body interaction term itself on the outcome of the renormalization group flow. This we do by alternatively including and excluding this vertex. That is, we solve the set $\{\mu, V_0, U_0\}$ and the set $\{\mu, V_0\}$ and compare the results we find. For that purpose, we plot in Fig. 3 the $p - n^{-1}$ -diagram near the critical density n_c , where the influence of U_0 is largest. From this figure we see that the change in density and pressure is about 1% at maximum. Far away from the critical conditions, i.e. at large negative chemical potential, the system becomes more and more dilute, and the influence of the U_0 term vanishes, consistent with expectations. In principle, we could choose to maintain the three-body interaction term in the renormalization group equations. However, as its effect is very small we will from now on neglect U_0 altogether. Thus, the dilute Bose gas, and more in particular the nonuniversal properties we are interested in, is accurately

described by only following the renormalization of the chemical potential and the two-body interaction. Having concluded this, we restrict ourselves from now on to the coupled Eqs. (13a) and (13b).

However, before we analyze some physical implications of these equations, we want to remark that the dependence on the ultraviolet cutoff Λ is indeed eliminated from the theory. The influence on e.g. the density can be shown to be completely absent, of course with the limitations that $\hbar\Lambda$ should be larger than the thermal momentum \hbar/Λ_{th} and that V_0 is properly renormalized to $4\pi a\hbar^2/m$ when we enter the thermal regime. We are going to compare the results from the renormalization group calculation with known results for the weakly-interacting Bose gas as found from the many-body T -matrix theory [15,32]. Far from the critical temperature we expect the results of the mean-field and renormalization group calculations to be identical. However, close to the critical temperature the renormalization group method will clearly deviate from mean-field theory. We will here focus on the behavior of the effective two-body interaction, and defer the discussions concerning the equation of state and other thermodynamic quantities to Sec. IV when we are able to describe also the condensed phase of the gas.

In the many-body T -matrix theory, the chemical potential is renormalized to $\mu' = \mu - 2nT^{2B}(\mathbf{0}, \mathbf{0}; 0)$ [32]. This is one of the results of including all two-body scattering processes, but also incorporating the effect of the medium on the scattering. Including the latter effect on the collisions in the gas, which was first carried out explicitly in Refs. [8], [15] and [32], is an important step forward in the correct mean-field treatment of the dilute Bose gas, since including many-body effects causes the effective interaction to go to zero at the critical temperature. This resolves a number of problems found in previous approaches using just the two-body scattering length a [16–19]. With our renormalization group approach we can corroborate this result and even go somewhat further than that. In our previous work we included only the many-body effects coming from the ladder diagrams. However, a class of diagrams that in principle also affects the two-body interaction are the bubble diagrams. With our current set of renormalization group equations we can precisely study

the effect of these bubble diagrams on the effective interaction. This is straightforward because we can pinpoint the ladder and bubble contributions in the equation describing the renormalization of the interaction. By alternatively including and excluding the bubble diagrams and then solving the renormalization group equations we can study the relative importance of the bubble diagrams on the effective ‘many-body’ scattering length a^{eff} . To avoid any confusion we will adopt the following notation for the scattering length. The normal ‘bare’ two-body scattering length as found e.g. from analysis of the appropriate association spectra is denoted by a , as usual. The effective scattering length a^{eff} includes also effects of the medium on two-body scattering, and therefore depends on the specific approximation used to calculate this effect. Here we consider two such approximations and denote the corresponding scattering lengths by a^{MB} and a^{RG} . In the first case it is the result of a many-body T -matrix calculation and is defined through $T^{MB}(\mathbf{0}, \mathbf{0}, \mathbf{0}; 0) = 4\pi a^{MB} \hbar^2 / m$. In the second case it is the result of a renormalization group calculation and is defined through $V_0(l = \infty) = 4\pi a^{RG} \hbar^2 / m$, irrespective of the fact if bubbles are or are not included in this calculation. In Fig. 4 we depict the ratio of the effective scattering length resulting from the renormalization group approach to the simple two-body scattering length a when we include and exclude the bubble diagrams, as a function of T/T_c and at a density of $1.5 \cdot 10^{12} \text{ cm}^{-3}$. We conclude that the effect of the bubbles can be rather large and is in particular important near the critical temperature. Further away from the critical temperature the importance of the bubbles rapidly decreases. This implies that calculating the influence of many-body effects by means of the ladder diagrams (i.e. doing the full many-body T -matrix calculation) can quantitatively give a poor estimate for a^{eff} . However, qualitatively there is clearly good agreement as we find from the renormalization group calculation that the effective scattering length indeed goes to zero at the critical temperature.

As already mentioned before, a bare chemical potential larger than the critical one, which is positive and yields a flow into the fixed point, corresponds to an inaccessible density regime. Therefore, we are not able to penetrate the region with a Bose condensate and cannot describe the Bose gas below the critical temperature with the renormalization group

equations in Eq. (13). Moreover, the critical exponent ν found from this set is not a very good approximation to the true value $\nu = 0.67$, even if we would include three-body interactions. These aspects are intimately related and due to the fact that in the case of a positive chemical potential, the $\mathbf{k} = \mathbf{0}$ part of the effective action has a Mexican hat shape. Therefore, we must explicitly break the symmetry and introduce the condensate density into the action by expanding the action around its minimum, and not around $\langle\psi\rangle = 0$ as was done in this section. For a negative chemical potential, the above approach is of course correct as then $\langle\psi\rangle$ is equal to zero.

IV. THE SYMMETRY BROKEN PHASE

Breaking the symmetry allows us to describe the dilute Bose gas below the critical temperature. Moreover, also above the critical temperature we find considerable improvement. This is due to the fact that a positive bare chemical potential can renormalize to negative values. Thus, starting out in the broken phase, the fluctuations can restore the symmetry and we end up in the unbroken phase above the critical temperature. The new set of renormalization group equations explicitly takes this broken symmetry into account and therefore gives a much better description than the one resulting from the set of equations in Eq. (13).

A. The flow equations

In order to expand the action around the correct extremum we have to perform the shift $a_{\mathbf{0},0} \rightarrow a_{\mathbf{0},0} + \sqrt{n_0 \hbar \beta V}$ which introduces the condensate density n_0 . Substituting this in the action Eq. (4) leads to the familiar expression [33]

$$\begin{aligned}
S[a, a^*] = & -\hbar\beta V(\mu n_0 - \frac{1}{2}n_0^2 V_0) + (-\mu\sqrt{n_0} + n_0\sqrt{n_0}V_0)(a_{\mathbf{0},0}^* + a_{\mathbf{0},0}) \\
& + \sum_{\mathbf{k},n} (-i\hbar\omega_n + \epsilon_{\mathbf{k}} - \mu + 2n_0 V_0) a_{\mathbf{k},n}^* a_{\mathbf{k},n} + \frac{1}{2}n_0 V_0 \sum_{\mathbf{k},n} (a_{\mathbf{k},n}^* a_{-\mathbf{k},-n}^* + a_{\mathbf{k},n} a_{-\mathbf{k},-n}) \\
& + \sqrt{\frac{n_0}{\hbar\beta V}} \sum_{\substack{\mathbf{k},\mathbf{q} \\ n,m}} V_0 (a_{\mathbf{q},m}^* a_{\mathbf{k}-\mathbf{q},n-m}^* a_{\mathbf{k},n} + a_{\mathbf{k}+\mathbf{q},n+m}^* a_{\mathbf{q},m} a_{\mathbf{k},n})
\end{aligned}$$

$$+ \frac{1}{2} \frac{1}{\hbar\beta V} \sum_{\substack{\mathbf{k}, \mathbf{k}', \mathbf{q} \\ n, n', m}} V_0 a_{\mathbf{k}+\mathbf{q}, n+m}^* a_{\mathbf{k}'-\mathbf{q}, n'-m}^* a_{\mathbf{k}', n'} a_{\mathbf{k}, n} , \quad (21)$$

for the action. The magnitude of the condensate is determined by eliminating the linear term from the action. In first instance we thus find $n_0 = \mu/V_0$. As a result, we can write the action as

$$\begin{aligned} S[a, a^*] &= -\hbar\beta V \omega_0 + \sum_{\mathbf{k}, n} (-i\hbar\omega_n + \epsilon_{\mathbf{k}} + \Gamma_{11}) a_{\mathbf{k}, n}^* a_{\mathbf{k}, n} + \frac{1}{2} \Gamma_{12} \sum_{\mathbf{k}, n} (a_{\mathbf{k}, n}^* a_{-\mathbf{k}, -n}^* + a_{\mathbf{k}, n} a_{-\mathbf{k}, -n}) \\ &+ \frac{\Gamma_3}{\sqrt{\hbar\beta V}} \sum_{\substack{\mathbf{k}, \mathbf{q} \\ n, m}} (a_{\mathbf{q}, m}^* a_{\mathbf{k}-\mathbf{q}, n-m}^* a_{\mathbf{k}, n} + a_{\mathbf{k}+\mathbf{q}, n+m}^* a_{\mathbf{q}, m} a_{\mathbf{k}, n}) \\ &+ \frac{1}{2} \frac{V_0}{\hbar\beta V} \sum_{\substack{\mathbf{k}, \mathbf{k}', \mathbf{q} \\ n, n', m}} a_{\mathbf{k}+\mathbf{q}, n+m}^* a_{\mathbf{k}'-\mathbf{q}, n'-m}^* a_{\mathbf{k}', n'} a_{\mathbf{k}, n} , \quad (22) \end{aligned}$$

introducing $\omega_0 = n_0^2 V_0/2$ as the lowest order approximation to the thermodynamic potential density, and defining the vertices $\Gamma_{11} = \mu - \hbar\Sigma_{11}(\mathbf{0}; 0)$, $\Gamma_{12} = \hbar\Sigma_{12}(\mathbf{0}; 0)$ and Γ_3 for which we have in lowest order that $\Gamma_{11} = \Gamma_{12} = n_0 V_0 = \mu$ and $\Gamma_3 = \sqrt{n_0} V_0 = \sqrt{\mu V_0}$. These are the boundary conditions for the flow equations we derive next.

Deriving the renormalization group equations using Feynman diagrams is in this case more involved than in the unbroken phase as the number of vertices is larger, but more so because we now also can have anomalous propagators $\langle a_{\mathbf{k}, n}^* a_{-\mathbf{k}, -n}^* \rangle$ and $\langle a_{\mathbf{k}, n} a_{-\mathbf{k}, -n} \rangle$ in these diagrams. The number of diagrams is therefore much larger and the combinatorics is more complicated. Therefore, we will here use a different method to obtain the renormalization group equations which does not explicitly make use of Feynman diagrams, and is therefore very useful and efficient in this case. It relies on the fact that in Eq. (7)

$$\int d[\psi_{>}^*] d[\psi_{>}] \exp \left\{ -\frac{1}{\hbar} (S_0[\psi_{>}^*, \psi_{>}] + S_I[\psi_{<}^*, \psi_{<}, \psi_{>}^*, \psi_{>}]) \right\} \equiv \exp \left\{ -Tr[\ln(-G_{>}^{-1})] \right\} , \quad (23)$$

where the trace is over Fourier modes in the shell $d\Lambda$ only and $G_{>}$ is the Greens function for these fast modes. Taking the shell infinitesimal again, we can simply calculate $\ln(-G_{>}^{-1})$ because we then only need the part of the total action which is quadratic in the fast Fourier modes (yielding all one-loop contributions). The coefficients of this quadratic part also contain the slow modes because the interaction term $S_I[\psi_{<}^*, \psi_{<}, \psi_{>}^*, \psi_{>}]$ couples the slow

and fast modes. By simply Taylor expanding $\ln(-G_{>}^{-1})$ we straightforwardly find the new effective action for the slow modes and the renormalization group equations of any vertex we would like to consider.

Thus, we split the fields in slow modes and fast modes as in Eq. (5) and find that the part from the action which is quadratic in the fast modes and only leads to the renormalization of coupling constants reads

$$\begin{aligned}
S^{(2)}[\psi_{>}^*, \psi_{>}] &= \sum'_{\mathbf{k},n} (-i\hbar\omega_n + \epsilon_{\mathbf{k}} + \Gamma_{11} + 2\Gamma_3(\psi_{<}^* + \psi_{<}) + 2V_{\mathbf{0}} |\psi_{<}|^2) a_{\mathbf{k},n}^* a_{\mathbf{k},n} \\
&+ \left(\frac{1}{2}\Gamma_{12} + \Gamma_3\psi_{<} + \frac{1}{2}V_{\mathbf{0}}\psi_{<}^2\right) \sum'_{\mathbf{k},n} a_{\mathbf{k},n}^* a_{-\mathbf{k},-n}^* \\
&+ \left(\frac{1}{2}\Gamma_{12} + \Gamma_3\psi_{<}^* + \frac{1}{2}V_{\mathbf{0}}\psi_{<}^{*2}\right) \sum'_{\mathbf{k},n} a_{\mathbf{k},n} a_{-\mathbf{k},-n} , \tag{24}
\end{aligned}$$

where the prime denotes that the sum over momenta is restricted to an infinitesimal momentum shell $d\Lambda$ at the cutoff. Evaluating the functional integral over these fast modes leads to adding $\text{Tr}(\ln(-G_{>}^{-1}))$ to the action for the slow fields, and thus changes the vertices. This quantity is most easily evaluated by performing a Bogoliubov transformation to diagonalize Eq. (24) [34], and we find that

$$\text{Tr}(\ln(-G_{>}^{-1})) = \frac{\Lambda^2}{2\pi^2} \left[\frac{1}{\beta} \ln(1 - e^{-\beta E_{\Lambda}}) + \frac{1}{2}(E_{\Lambda} - (\epsilon_{\Lambda} + \Gamma_{11} + 2\Gamma_3(\psi_{<}^* + \psi_{<}) + 2V_{\mathbf{0}} |\psi_{<}|^2)) \right] d\Lambda , \tag{25}$$

where the second term originates from the diagonalization procedure, and the ‘dispersion’ E_{Λ} is found from

$$\begin{aligned}
E_{\Lambda}^2 &= (\epsilon_{\Lambda} + \Gamma_{11} + 2\Gamma_3(\psi_{<}^* + \psi_{<}) + 2V_{\mathbf{0}} |\psi_{<}|^2)^2 - \\
&(\Gamma_{12} + \Gamma_3\psi_{<} + \frac{1}{2}V_{\mathbf{0}}\psi_{<}^2)(\Gamma_{12} + \Gamma_3\psi_{<}^* + \frac{1}{2}V_{\mathbf{0}}\psi_{<}^{*2}) . \tag{26}
\end{aligned}$$

In zeroth order in $\psi_{<}$ and $\psi_{<}^*$ we retrieve the well-known Bogoliubov dispersion $\hbar\omega_{\Lambda} = \sqrt{(\epsilon_{\Lambda} + \Gamma_{11})^2 - \Gamma_{12}^2}$, equal to $\hbar\omega_{\Lambda} = \sqrt{\epsilon_{\Lambda}^2 + 2\Gamma_{11}\epsilon_{\Lambda}}$ and thus gapless at $l = 0$ due to the equality $\Gamma_{11}(l = 0) = \Gamma_{12}(l = 0)$. This corresponds to the Hugenholtz-Pines theorem [35]. Performing a Taylor expansion in terms of the slow modes we find the new action. Thus, integrating out a momentum shell renormalizes the existing vertices, but also generates new

terms in the action, and in particular a linear term. To eliminate this term and remain in the minimum of the action we again have to perform a small shift in $a_{\mathbf{0},0}$. This implies that the magnitude of the condensate changes as we are integrating out momentum shells and we also have a flow equation for the condensate density. Since we omit three-body interactions containing six fields, we also have to neglect terms containing five fields since they correspond, together with the condensate field, with a three-body term. As a result, the action remains of the form written down in Eq. (22) and the renormalization group equations can now be obtained for all the vertices of interest. However, due to the $U(1)$ -symmetry of our problem, we can relate some of these vertices and thereby limit the number of flow equations we actually need to describe the complete renormalization of the action in Eq. (22). As this $U(1)$ -symmetry cannot be broken during the process of renormalization, the action can, at any time, be recast in the explicitly $U(1)$ symmetric form

$$S'[\psi_{<}^*, \psi_{<}] = \int_0^{\hbar\beta} d\tau \int d\mathbf{x} \left(\psi_{<}^*(\mathbf{x}, \tau) \left[\hbar \frac{\partial}{\partial \tau} - \frac{\hbar^2 \nabla^2}{2m} - \mu(l) \right] \psi_{<}(\mathbf{x}, \tau) + \frac{1}{2} V_{\mathbf{0}}(l) |\psi_{<}(\mathbf{x}, \tau)|^4 \right). \quad (27)$$

From this it is then first of all easy to see that the Hugenholtz-Pines theorem [35] holds, implying that $\Gamma_{11}(l) = \Gamma_{12}(l) = \mu(l)$. (See appendix A for an explicit derivation of this important relation.) Next, also due to the neglect of three-body interactions, we have that $\Gamma_3(l) = \sqrt{n_{\mathbf{0}}(l)} V_{\mathbf{0}}(l)$ and $V_{\mathbf{0}}(l) = \Gamma_{12}(l)/n_{\mathbf{0}}(l)$. Thus, we only need to know the flow equations for e.g. $n_{\mathbf{0}}(l)$ and $\Gamma_{12}(l)$ and then the other renormalization group equations can be determined. In the following we can therefore restrict ourselves to the renormalization of the linear term and the term proportional to $(\psi_{<}^{*2} + \psi_{<}^2)$ as these determine the change of the condensate density and the anomalous selfenergy Γ_{12} respectively. Note that the equality $\Gamma_{11}(l) = \Gamma_{12}(l)$ ensures that the dispersion $\hbar\omega_{\Lambda}$ is gapless at any point during renormalization, as it should.

To arrive at the flow equations for $n_{\mathbf{0}}(l)$ and $\Gamma_{12}(l)$, we first of all need the linear term $d\Gamma_0(a_{\mathbf{0},0}^* + a_{\mathbf{0},0})$ that is generated by integrating out a momentum shell. We find that

$$d\Gamma_0 = \frac{\Lambda^3}{2\pi^2} \left(\frac{2\Gamma_3(\epsilon_{\Lambda} + \Gamma_{11} - \frac{1}{2}\Gamma_{12})}{\hbar\omega_{\Lambda}} N(\hbar\omega_{\Lambda}) + \frac{1}{2} \left(\frac{2\Gamma_3(\epsilon_{\Lambda} + \Gamma_{11} - \frac{1}{2}\Gamma_{12})}{\hbar\omega_{\Lambda}} - 2\Gamma_3 \right) \right) dl. \quad (28)$$

Analogously we find a change $d\Gamma_{12}^{(0)}$ in the anomalous selfenergy. (See appendix A for details.) However, before we know the full renormalization of this vertex we have to determine the shift needed to eliminate the linear term that is generated. Substituting $a_{\mathbf{0},0} \rightarrow a_{\mathbf{0},0} + \sqrt{\hbar\beta V}d(\sqrt{n_{\mathbf{0}}})$ and retaining only the term linear in $d(\sqrt{n_{\mathbf{0}}})$ we find that

$$d(\sqrt{n_{\mathbf{0}}}) = -\frac{d\Gamma_{\mathbf{0}}}{\Gamma_{11} + \Gamma_{12}} \quad (29)$$

which influences the renormalization of Γ_{12} because we have for the total renormalization of the anomalous selfenergy

$$d\Gamma_{12} = d\Gamma_{12}^{(0)} + 2\Gamma_3 d(\sqrt{n_{\mathbf{0}}}) . \quad (30)$$

due to this shift. Using the above mentioned relations between the vertices implicate from the $U(1)$ -symmetry we then make contact with the renormalization group equations for the unbroken phase by determining the flow equations for the chemical potential $\mu = \Gamma_{12}$ and the two-body interaction $V_{\mathbf{0}} = \Gamma_{12}/n_{\mathbf{0}}$. After some algebra we ultimately find

$$\frac{d\mu}{dl} = 2\mu - \frac{\Lambda^3}{2\pi^2}V_{\mathbf{0}} \left[\frac{2\epsilon_{\Lambda}^3 + 6\mu\epsilon_{\Lambda}^2 + \mu^3}{2\hbar^3\omega_{\Lambda}^3}(2N(\hbar\omega_{\Lambda}) + 1) - 1 + \frac{\mu(2\epsilon_{\Lambda} + \mu)^2}{\hbar^2\omega_{\Lambda}^2}\beta N(\hbar\omega_{\Lambda})[N(\hbar\omega_{\Lambda}) + 1] \right] \quad (31a)$$

$$\frac{dV_{\mathbf{0}}}{dl} = -V_{\mathbf{0}} - \frac{\Lambda^3}{2\pi^2}V_{\mathbf{0}}^2 \left[\frac{(\epsilon_{\Lambda} - \mu)^2}{2\hbar^3\omega_{\Lambda}^3}(2N(\hbar\omega_{\Lambda}) + 1) + \frac{(2\epsilon_{\Lambda} + \mu)^2}{\hbar^2\omega_{\Lambda}^2}\beta N(\hbar\omega_{\Lambda})[N(\hbar\omega_{\Lambda}) + 1] \right] , \quad (31b)$$

and the condensate density follows from $n_{\mathbf{0}}(l) = \mu(l)/V_{\mathbf{0}}(l)$. Breaking the symmetry is irrelevant to the trivial scaling of the vertices, and thus these are identical to what was found in the previous section. Comparing these flow equations to Eqs. (13a) and (13b) omitting $U_{\mathbf{0}}$, we see that both sets coincide when μ is taken equal to zero. Thus, the renormalization group equations for negative and positive chemical potential yield a flow which is continuously differentiable, also at $\mu = 0$.

We now know the renormalization of the chemical potential and the two-body interaction. Finally, we again have to find the equations describing the building up of the total and superfluid densities and the thermodynamic potential as we are integrating out momentum

shells. Analogous to the procedure followed in the previous section we find for the total density, being the sum of the condensate density and the above condensate density,

$$\frac{dn}{dl} = -\frac{\Lambda^3}{2\pi^2} \left(\frac{\epsilon_\Lambda}{2\hbar\omega_\Lambda} (2N(\hbar\omega_\Lambda) + 1) - \frac{1}{2} \right) e^{-3l} \quad (32)$$

with the boundary condition $n(l=0) = n_0(l=0) = \mu(l=0)/V_0(l=0)$. The superfluid density follows from

$$\frac{dn_s}{dl} = \frac{dn}{dl} - \frac{\Lambda^3}{3\pi^2} \beta \epsilon_\Lambda N(\hbar\omega_\Lambda) [N(\hbar\omega_\Lambda) + 1] e^{-3l} , \quad (33)$$

and the thermodynamic potential from

$$\frac{d\omega}{dl} = \frac{\Lambda^3}{2\pi^2} \left(\frac{1}{\beta} \ln(1 - e^{-\beta\hbar\omega_\Lambda}) e^{-5l} + \frac{1}{2} (\hbar\omega_\Lambda - \epsilon_\Lambda - \mu) e^{-3l} \right) , \quad (34)$$

(cf. Eq. (25)) with the boundary condition $\omega(l=0) = \omega_0 = n_0^2 V_0/2$.

B. The critical temperature of BEC

With the boundary conditions mentioned above we can again numerically integrate the renormalization group equations. For a fixed temperature, we vary the value of the (positive) bare chemical potential, and calculate e.g. density and pressure. The physical effective chemical potential, i.e. with the trivial scaling removed, decreases as we perform the integration, and depending on the starting value remains positive, renormalizes exactly to zero, or becomes negative at some value of the integration parameter l . In the first case we start out and remain in the broken phase and are below the critical temperature of Bose-Einstein condensation, i.e. we have a finite condensate density. In the second case, the condensate density $n_0(l) = \mu(l)/V_0(l)$ renormalizes exactly to zero for $l \rightarrow \infty$, and we are at the critical conditions for Bose-Einstein condensation. In the third case we started out in the broken phase, but the fluctuations restore the symmetry. At the value of l for which the chemical potential becomes negative we have to continue the integration with the set Eqs. (13a) and (13b), and we are thus in the uncondensed phase. Hence, to be able to describe the dilute Bose gas above, but not too far from the critical temperature, we need the renormalization

group equations for both signs of μ . In Fig. 5 we depict the trajectories resulting from the integration of Eqs. (31a) and (31b).

It is evident from this figure that the critical properties of the Bose gas are determined by this set of equations. By linearizing the flow equations around the fixed point we can identify the largest eigenvalue λ_+ , and determine the critical exponent ν following from this set. We find $\nu = 0.685$, which gives a much better approximation to the critical exponent than the renormalization group equations studied in Sec. III and is to be compared with the value $\nu = 0.67$ found from the ϵ -expansion of the $O(2)$ model [31] and measured in ^4He experiments. The agreement is surprisingly good, and together with the fact that we explicitly showed that three-body effects are negligible, this indicates that we are indeed accurately describing the Bose gas with the derived renormalization group equations, also in the critical region. The cause of this good agreement is that although we only consider the renormalization of μ and $V_{\mathbf{0}}$, the type of scattering processes in terms of real (bare) particles we are actually taking into account are very elaborate. The propagator for the the Bogoliubov quasiparticles is namely the result of dressing the original bare propagator $\hbar/(i\hbar\omega_n - \epsilon_{\Lambda} + \mu)$ with interactions with the condensate as we use the terms $2n_{\mathbf{0}}V_{\mathbf{0}}a_{\mathbf{k},n}^*a_{\mathbf{k},n}$ and $n_{\mathbf{0}}V_{\mathbf{0}}(a_{\mathbf{k},n}^*a_{-\mathbf{k},-n}^* + a_{\mathbf{k},n}a_{-\mathbf{k},-n})/2$ in the zeroth order quadratic part of the action. Thus, the diagrams we calculate actually contain an infinite number of scattering processes with the condensate. Therefore, we are describing the system much better than in Sec. III already at this level of renormalization group.

The first nonuniversal property we concentrate on is the change in the critical temperature of Bose-Einstein condensation due to interaction effects. This result is presented also elsewhere [20], but we will recapitulate it here because of its experimental significance. At fixed temperatures we vary the (bare) chemical potential to find the trajectories flowing into the fixed point. Using Eq. (32), this yields the critical densities for these specific temperatures and gives us the $n_c - T$ relation at which Bose-Einstein condensation occurs. We repeat this for different values of the scattering length to obtain the dependence of the critical temperature on the strength of the interaction. In Fig. 6 we show the degeneracy

parameter $n_c \Lambda_{th}^3$ found from the renormalization group calculation as a function of a/Λ_{th} . As seen from this figure we conclude that the critical temperature is *raised* with respect to the ideal gas value. This is in qualitative agreement with the recent experiments [1,2] and also preliminary Quantum Monte Carlo calculations seem to confirm this result [36]. An indication of an upward shift was also found some time ago by one of us studying the nucleation of Bose-Einstein condensation [8]. From our calculations we predict that for the ^{87}Rb and ^{23}Na experiments the critical temperature can be raised with as much as 10 %, which appears to be a very promising result because one might expect that an effect of this magnitude can very well be measured in future, more accurate, experiments. It is important to note that this shift in $n_c \Lambda_{th}^3$ can be observed in magnetically trapped atomic gases if one directly measures the density in the center of the trap at the critical temperature. One should in particular *not* measure the total number of particles, because this involves the density profile in the trap and due to the repulsive nature of the interactions thus tends to obscure the effect [37].

The reason for a higher critical temperature, or more precisely, a lower critical density is the following. The effective chemical potential renormalizes from a positive initial value exactly to zero. Consequently, we have the Bogoliubov dispersion in the equation for the density, and this depresses the occupation of the non-zero momentum states relative to the ideal gas case, where we would just have ϵ_Λ in the Bose-Einstein distribution function. The magnitude of the effect is related to the behavior of the chemical potential when renormalizing to the fixed point value $\mu^* = \epsilon_\Lambda$. Suppose we effectively have $\mu(l) = \alpha \epsilon_\Lambda$ independent of l , with some positive α smaller than 1. We can then translate the differential equation for the density into an ordinary integral over momentum space following the inverse procedure from which we found the flow equations in Sec. III. Doing so, we find that the Bogoliubov dispersion effectively becomes $\hbar\omega_{\mathbf{k}} = \sqrt{1 + 2\alpha\epsilon_{\mathbf{k}}}$. Thus, this essentially boils down to a mass renormalization, and the change in the critical temperature is directly related to the magnitude of this renormalization. Starting with the equation describing the building up of the above condensate density (cf. Eq. (A.6a) from appendix A) one can easily show that we

approximately have $n_c \Lambda_{th}^3 = (1 + \alpha)g_{3/2}(1)/(1 + 2\alpha)$. For an increase of 10 % in the critical temperature, we find from this result that α must be equal to 0.2. Indeed, this turns out to be the typical value of α in the thermal regime where the contributions to the density are largest.

C. The region $na\Lambda_{th}^2 \ll 1$

To obtain also information on the properties of the Bose gas below the critical temperature we have to start with a chemical potential which always remains positive under renormalization. We are then always in the condensed phase and have to use the renormalization group equations (31a) and (31b). Written as ordinary one-loop integrals, these equations contain infrared divergencies and a straightforward perturbative analysis is not possible. This is a well known problem in the theory of the interacting Bose gas [38,39]. However, doing the calculation by means of the renormalization group approach, this problem is in principle resolved due to the resummation which is automatically performed. The presence of infrared divergencies causes both the physical chemical potential and two-body interaction in the renormalization group approach to renormalize to zero, instead of becoming infinite as they would in a regular one-loop calculation. Indeed, one can show from Eqs. (31a) and (31b) that for $l \rightarrow \infty$ we have $\mu \propto e^l$ and $V_0 \propto e^{-2l}$. These scalings are different from the trivial scalings $\mu \propto e^{2l}$ and $V_0 \propto e^{-l}$, and are therefore termed anomalous. Physically, the anomalous scaling implies an effective energy and momentum dependence of the coupling constants, as we show explicitly in appendix B. In particular, the anomalous scaling we find leads to the result that the chemical potential, and thus the normal and anomalous selfenergies, as well as the two-body interaction, behave linearly with k for low momenta, i.e. our renormalization group approach reveals that $\hbar\Sigma_{11}(\mathbf{k}; 0) \propto k$ and $\hbar\Sigma_{12}(\mathbf{k}; 0) \propto k$. This behavior, implying that $\hbar\Sigma_{11}(\mathbf{0}; 0) = \hbar\Sigma_{12}(\mathbf{0}; 0) = 0$, is an exact result for low momenta [39] which we explicitly recover here. The consequences for the application of renormalization group are however twofold. First, it implies that the Bogoliubov dispersion $\hbar\omega_{\mathbf{k}}$ does not

possess a sound mode anymore since the low momentum behavior is not linear, but instead we have $\hbar\omega_{\mathbf{k}} \propto k^{3/2}$. This is of course an incorrect result [38] indicating that Eqs. (31a) and (31b) are insufficient to describe the sound mode. Indeed, following the argument in Sec. III we neglected the renormalization of the (marginal) $\partial/\partial\tau$ and $|\nabla|^2$ terms since the interactions were anticipated to be momentum and energy independent. However, below the critical temperature we see that the momentum and energy dependence of the selfenergies does become important, and should therefore be included in the renormalization group calculation by Taylor expanding the selfenergies in terms of the external momentum and frequency. Put differently, the anomalous dimension η is no longer small below the critical temperature. The extra renormalization group equations obtained in this manner may change the particular anomalous scaling found above, but since $\hbar\Sigma_{11}(\mathbf{0};0) = \hbar\Sigma_{12}(\mathbf{0};0) = 0$ is an exact result we still expect to have anomalous scaling of the coupling constants. The effect of the extra renormalization group equations will be to change the dispersion relation in such a way that the linear sound mode is recovered. We will not pursue this calculation here, but postpone it to future work.

The reason for the anomalous scaling and consequently the disappearance of the sound mode, is caused by the infrared divergence in the one-loop expressions for the selfenergies and two-body interaction. This can be traced back to the behavior of the coherence factors $u_{\mathbf{k}}$ and $v_{\mathbf{k}}$ of the Bogoliubov transformation diagonalizing the quadratic part of the action. The Bogoliubov transformation is given by

$$a_{\mathbf{k},n} = u_{\mathbf{k}}b_{\mathbf{k},n} - v_{\mathbf{k}}b_{-\mathbf{k},-n}^*, \quad (35a)$$

$$a_{\mathbf{k},n}^* = u_{\mathbf{k}}b_{\mathbf{k},n}^* - v_{\mathbf{k}}b_{-\mathbf{k},-n}, \quad (35b)$$

where $b_{\mathbf{k},n}^*$ and $b_{\mathbf{k},n}$ are the Fourier components of the fields creating respectively annihilating a Bogoliubov quasiparticle. The coherence factors are given by

$$u_{\mathbf{k}} = \frac{1}{2} \left(\sqrt{\frac{\hbar\omega_{\mathbf{k}}}{\epsilon_{\mathbf{k}}}} + \sqrt{\frac{\epsilon_{\mathbf{k}}}{\hbar\omega_{\mathbf{k}}}} \right), \quad (36a)$$

$$v_{\mathbf{k}} = \frac{1}{2} \left(\sqrt{\frac{\hbar\omega_{\mathbf{k}}}{\epsilon_{\mathbf{k}}}} - \sqrt{\frac{\epsilon_{\mathbf{k}}}{\hbar\omega_{\mathbf{k}}}} \right), \quad (36b)$$

and satisfy the requirement that $u_{\mathbf{k}}^2 - v_{\mathbf{k}}^2 = 1$ because the Bogoliubov transformation is unitary. As the Bogoliubov dispersion is given by $\hbar\omega_{\mathbf{k}} = \sqrt{\epsilon_{\mathbf{k}}^2 + 2\mu\epsilon_{\mathbf{k}}}$, it is easy to see that $u_{\mathbf{k}} \rightarrow 1$ and $v_{\mathbf{k}} \rightarrow 0$ for large momenta, and both factors behave as $1/\sqrt{k}$ as k tends to zero. The region where the crossover occurs between these two regimes is determined by the parameter $na\Lambda_{th}^2$, found from comparing the chemical potential with the thermal energy, and also determining the crossover from quadratic to linear behavior of the Bogoliubov dispersion. When $na\Lambda_{th}^2 \gg 1$ the linear regime of the dispersion is extremely important in determining the properties of the Bose gas. Conversely, when $na\Lambda_{th}^2 \ll 1$, the Bogoliubov dispersion can be approximated by the normal dispersion $\epsilon_{\mathbf{k}} + \mu$, except for a very small region at low momenta, which is then not very important and can for most practical purposes be neglected. In the following, we therefore concentrate on the regime $na\Lambda_{th}^2 \ll 1$, covering a large temperature interval below the critical temperature, and use $u_{\mathbf{k}} = 1$ and $v_{\mathbf{k}} = 0$ in contributions to the renormalization of the vertices that contain infrared divergencies. Otherwise, we will use the full expression Eq. (36). This procedure turns out to be necessary to ensure the Hugenholtz-Pines theorem to be satisfied, as is shown in appendix A.

In the method used in the previous section it is not possible to pinpoint the Bogoliubov coherence factors at any stage of the derivation of the renormalization group equations. Therefore, we really have to go through the calculation of the Feynman diagrams relevant to the various vertices we are interested in. In our case these are the linear term of the action and the anomalous selfenergy. The one-loop diagrams of interest are depicted in Fig. 7 and contain also the anomalous propagators $\langle a_{\mathbf{k},n}^* a_{-\mathbf{k},-n}^* \rangle$ and $\langle a_{\mathbf{k},n} a_{-\mathbf{k},-n} \rangle$. Using the Bogoliubov transformation, these diagrams are straightforward to calculate, and we find that for the renormalization of the condensate density both diagrams for Γ_0 contribute, but that for the renormalization of the anomalous selfenergy only diagrams *A* and *B* give contributions that do not contain infrared divergencies. The explicit calculation of these diagrams is presented in appendix A. Using the expressions obtained there, we find that the flow equations become

$$\frac{d\mu}{dl} = 2\mu - \frac{\Lambda^3}{2\pi^2} V_0 \left(\frac{\epsilon_\Lambda + \mu}{\hbar\omega_\Lambda} (2N(\hbar\omega_\Lambda) + 1) - 1 + 4\beta\mu N(\hbar\omega_\Lambda) [N(\hbar\omega_\Lambda) + 1] \right), \quad (37a)$$

$$\frac{dV_0}{dl} = -V_0 - \frac{\Lambda^3}{2\pi^2} V_0^2 \left(\frac{1 + 2N(\hbar\omega_\Lambda)}{2\hbar\omega_\Lambda} + 4\beta N(\hbar\omega_\Lambda) [N(\hbar\omega_\Lambda) + 1] \right), \quad (37b)$$

where we again made use of the relations $\mu(l) = \Gamma_{11}(l) = \Gamma_{12}(l) = \sqrt{n_0(l)}\Gamma_3(l) = n_0(l)V_0(l)$ due to $U(1)$ -symmetry. Note that also this set coincides with Eqs. (13a) and (13b) when the chemical potential is equal to zero, so the flow is also in this case everywhere continuous and continuously differentiable. Moreover, the equations for the density, superfluid density and thermodynamic potential do not contain an infrared divergency, so the flow equations for these quantities remain the same and are given by Eqs. (32), (33) and (34), respectively.

D. Analysis of the flow equations

At this point we can describe any point in the phase diagram of the dilute Bose gas. For negative chemical potential we have Eqs. (13a) and (13b), for positive chemical potential we must use Eqs. (37a) and (37b). Moreover, we have to combine both sets when we are not too far below the critical density when the chemical potential changes sign during application of the renormalization group transformation. Using Eq. (37), we find that the critical temperature of Bose-Einstein condensation changes with less than 0.1 % compared to the more accurate result found using Eq. (31). Therefore, this shows that using the set not containing the infrared divergencies essentially leads to the same results, implying that it is indeed correct to neglect the linear part of the Bogoliubov dispersion. Having proven this explicitly, we will in the following present the results of the renormalization group calculation of the effective two-body interaction, i.e. the many-body scattering length a^{eff} , the condensate and superfluid densities and the $p - n^{-1}$ -diagram below as well as above the critical temperature, and compare them in all cases with the results from the many-body T -matrix calculation.

We start with the scattering length a^{eff} . Above the critical temperature it is straightforward to take into account only the contributions of the ladder diagrams, or to include

the effect of the bubble diagrams as well. Below the critical temperature there are no clear ladder and bubble diagrams, so the various contributions are in principle not clearly associated with ladders or bubbles. However, comparing the differential equations for positive and negative μ we can conclude that the first nontrivial term on the righthand side of Eq. (37b) is effectively related to a ladder contribution, and that the second nontrivial term is effectively related to a bubble diagram. We depict in Fig. 8 the scattering length a^{eff} , normalized to the two-body scattering length $a = 52a_0$ for ^{23}Na , when including and excluding the bubble contributions (a^{RG}/a), and also the result found from the many-body T -matrix calculation (a^{MB}/a) [15]. As our approach is restricted to the regime $na\Lambda_{th}^2 \ll 1$, we present no results for $na\Lambda_{th}^2$ larger than one. The renormalization of the effective two-body interaction to zero at the critical temperature, a result already found in the many-body T -matrix approach, turns out to be correct. Indeed, this can be easily understood from the renormalization group equations. A fixed point (μ^*, V_0^*) is present in the set $\{\mu(l), V_0(l)e^{2l}\}$, which means that for $l \rightarrow \infty$ the physical two-body interaction, i.e. with the trivial scaling removed, behaves as $V_0^*e^{-l}$ and thus goes to zero. The depression in the scattering length around the critical temperature occurs in a fairly large temperature interval. Note furthermore that applying the renormalization group equations (31a) and (31b) would lead to $a^{RG} = 0$ everywhere below the critical temperature due to the anomalous scaling found from this set. This property is actually expected to hold true even in a more elaborate renormalization group calculation and is an issue worthwhile studying as it may have important consequences for e.g. the exact form of the Gross-Pitaevskii equation describing the condensate.

Next, we turn to the equation of state. For the ideal Bose gas we have in general that

$$n\Lambda_{th}^3 = n_0\Lambda_{th}^3 + g_{3/2}(\zeta) \quad (38)$$

where $g_n(z)$ is a Bose-function defined as

$$g_n(z) = \frac{1}{\Gamma(n)} \int_0^\infty \frac{y^{n-1}}{z^{-1}e^y - 1} dy \quad (39)$$

and $\zeta = e^{\beta\mu}$ the fugacity. In the many-body T -matrix theory above the critical temperature we have that the chemical potential is renormalized to $\mu' = \mu - 2nT^{2B}(\mathbf{0}, \mathbf{0}; 0)$ [32]. Below the

critical temperature the dispersion changes to the Bogoliubov dispersion and the equation for the density is in essence given by Eq. (32), recast in the form of an ordinary one-loop integral. In Fig. 9 we plot $n\Lambda_{th}^3$ for the ideal Bose gas, following from the many-body T -matrix calculation, and from the renormalization group calculation. In the latter case, we numerically integrate the flow equations for a fixed temperature, and vary the value of the bare chemical potential. This changes the total density in the system, and therefore the value of $n\Lambda_{th}^3$. For the ideal Bose gas, positive values of the chemical potential are not allowed. With the repulsive interactions taken into account, a positive value is possible and the fugacity can be larger than one. The renormalization group calculation yields the same density for a chemical potential slightly above and slightly below the critical chemical potential. This double valuedness in the density occurs in an extremely small region around the critical density and the effect is smaller than 1 promille in the case of ^{23}Na . For ^1H , with a scattering length $a = 1.34a_0$, the effect is even far below the promille level. However, it is important to note that this effect is much smaller than the change in density we obtain when we include three-body interactions, being approximately 1 % (cf. Sec. III). Therefore, the double valuedness we find cannot be trusted physically and should be neglected. It presumably disappears when we include three-body effects or extend the renormalization group calculation otherwise.

When the bare chemical potential decreases the gas becomes more and more dilute and the influence of the interactions can better and better be accounted for using mean-field theory. This fact is actually evident from the renormalization group equations in Eq. (13). When the chemical potential is large and negative, the Bose-factors $N(\epsilon_\Lambda - \mu)$ are strongly depressed and there is hardly any many-body effect on the renormalization of the two-body interaction so we will find that it is just renormalized to $T^{2B}(\mathbf{0}, \mathbf{0}; 0) = 4\pi a\hbar^2/m$. Indeed, the same is true in the many-body T -matrix calculation [15], since we have that $T^{MB}(\mathbf{0}, \mathbf{0}, \mathbf{0}; 0) \approx T^{2B}(\mathbf{0}, \mathbf{0}; 0)$ when the system is extremely dilute, i.e. there is no effect of the medium in this regime. In addition, the differential equations for μ and $V_{\mathbf{0}}$ are now almost decoupled, and consequently the chemical potential will renormalize approximately

to $\mu - 2nT^{2B}(\mathbf{0}, \mathbf{0}; 0)$, which is only a small effect in this limit. Therefore, the renormalization group equations can practically be recast in the regular one-loop expressions one encounters in the many-body T -matrix theory and the results we find in this regime are approximately the same.

In Figs. 10(a) and 10(b) we depict the condensate and superfluid fractions as a function of temperature for a density of $1.5 \cdot 10^{12} \text{ cm}^{-3}$ both from the renormalization group and many-body T -matrix calculation. Again, not too close to the critical temperature we have good agreement. Note that the superfluid density has not yet become zero at the temperature where the condensate density vanishes. To explain this aspect we will focus on the equation for the superfluid density in the unbroken phase. When we interpret the fact that the chemical potential is renormalized as we integrate out momentum shells as a chemical potential depending on momentum, we can express the superfluid density as a regular integral over momentum space, i.e.

$$n_s = \int \frac{d^3\mathbf{k}}{(2\pi)^3} \frac{1}{e^{\beta(\epsilon_{\mathbf{k}} - \mu(k))} - 1} - \int \frac{d^3\mathbf{k}}{(2\pi)^3} \frac{2}{3} \beta \epsilon_{\mathbf{k}} \frac{e^{\beta(\epsilon_{\mathbf{k}} - \mu(k))}}{(e^{\beta(\epsilon_{\mathbf{k}} - \mu(k))} - 1)^2}. \quad (40)$$

Writing $\mu(k) = \mu_0 + \delta\mu(k)$ and performing a Taylor expansion, we find to first order in $\delta\mu$ that

$$n_s = \int \frac{d^3\mathbf{k}}{(2\pi)^3} \beta N(\epsilon_{\mathbf{k}} - \mu_0) [N(\epsilon_{\mathbf{k}} - \mu_0) + 1] \left[1 - \frac{2}{3} \beta \epsilon_{\mathbf{k}} (2N(\epsilon_{\mathbf{k}} - \mu_0) + 1)\right] \delta\mu(k), \quad (41)$$

where the lowest order terms drop out. This is due to the fact that these terms yield the expression for the superfluid density in an ideal Bose gas above the critical temperature which can be shown to be exactly equal to zero. It is clear from Eq. (41) that the superfluid density will in general not be equal to zero. The behavior of $\delta\mu(k)$ would have to be very special to give a superfluid density exactly equal to zero. It is therefore not surprising that we find from our limited set of renormalization group equations a different temperature for which the condensate and superfluid densities vanish. For the situation depicted in Fig. 10 we have however that $\Delta T/T_c$ is only about $8 \cdot 10^{-3}$. Extending the renormalization group calculation would in principle lead to a superfluid density which vanishes at the same temperature as where the condensate density becomes zero.

Finally, we also present the pressure of the dilute Bose gas as a function of the inverse density. Using Eq. (34), we depict this behavior in Fig. 11 for a ^{23}Na gas at $1\ \mu\text{K}$, together with the result of the many-body T -matrix calculation. Although the critical densities are different, we find a fairly good agreement between the two curves and the difference between the renormalization group calculation and the many-body T -matrix calculation is small when it concerns the pressure of the gas. However, concerning the other nonuniversal properties discussed in this article, the difference can be substantial near the critical temperature as we have seen.

V. CONCLUSIONS

In summary, we have derived the renormalization group equations for a dilute Bose gas. To obtain these equations we have to make a distinction between the case of a negative and a positive chemical potential. In the latter case we have to take the presence of a condensate into account, and the renormalization group equations are different from the ones valid in the unbroken phase. Our philosophy of using the renormalization group approach is not to study universal properties of the dilute Bose gas, which are the same as for the $O(2)$ -model in three dimensions, but to make quantitative predictions about various nonuniversal properties of this system. To achieve this goal one has to find a method to eliminate the ultraviolet cutoff dependence inherent to the application of the renormalization group. Our knowledge about the two-body scattering problem is sufficient in this respect and we can fix the renormalization group equations in this manner. We compared results of the renormalization group with mean-field calculations and showed the difference to vanish in appropriate limits. We also checked the influence of three-body effects, which turned out to be unimportant even in the critical region. Furthermore, we showed that the influence of bubble diagrams on the effective interaction can be fairly large, and that the effective scattering length a^{eff} vanishes when approaching the critical temperature. This confirms earlier results [20,32] and is of importance for a lot of current work concerning condensate

properties in trapped Bose gases. It implies that there can in principle be an important change in the results of calculations that make use of the nonlinear Schrödinger equation when determining these properties. For that purpose the effective scattering length a^{eff} is of importance, and not the two-body scattering length a .

Next, we derived the renormalization group equations in the broken phase, i.e. for positive chemical potential, and showed that the transition to the Bose-Einstein condensed phase is contained in this set of renormalization group equations. We found a critical exponent $\nu = 0.685$, which agrees very well with $\nu = 0.67$ found in studies of the $O(2)$ -model, and furthermore calculated the effect of the interactions on the critical temperature of the phase transition. The change can be as much as 10 % in the current type of experiments and may be measured if one can improve the precision in determining the temperature and the central density in the trap.

As these latter renormalization group equations lead to a dispersion relation which has no linear part, i.e. there is no sound mode, we have to restrict ourselves to the regime $na\Lambda_{th}^2 \ll 1$, where the linear part of the dispersion is unimportant for determining properties such as density and pressure. The region where $na\Lambda_{th}^2 \ll 1$ is currently still the most interesting one from the experimental point of view although the other region is certainly within reach. Including the renormalization of the time derivative and gradient terms in the action is expected to resolve the problem of the disappearing of the sound mode, but we postponed this to future work. A resolution of this problem would correspond to a resolution of the long standing problem of the infrared divergencies in the perturbation expansion around the Bogoliubov theory.

We concluded this work with using the renormalization group to calculate superfluid and condensate densities as a function of temperature and also a $p - n^{-1}$ -diagram is presented. Of course the renormalization group can be used to find out many more things about the dilute Bose gas. Note e.g. that it is in principle also possible to use the renormalization group method to find the quantitative form of the correlation function as it is the Fourier transform of the occupation number $N_{\mathbf{k}}$. This can also be translated into a differential equation as in

Eq. (19) where we now have the distance r as a free parameter. Also the specific heat may be calculated. In principle, our results pertain to a homogeneous Bose gas, but in situations where the application of a local density approximation is allowed, they are also applicable to trapped Bose gases. Moreover, we indicated that it is in principle also possible to set up a renormalization group calculation for the inhomogeneous case.

Finally, we want to note that the procedure of renormalization group as described in this article can in principle also be used to study the Kosterlitz-Thouless transition to the superfluid phase in a two-dimensional Bose gas. However, there are difficulties in this case connected with the fact that all coupling constants are relevant at the critical temperature. Nonetheless, work along these lines is in progress since a number of experiments are currently under construction which aim at reaching the Kosterlitz-Thouless phase in doubly spin-polarized atomic hydrogen adsorbed on a superfluid helium film.

ACKNOWLEDGMENTS

We acknowledge helpful discussions with Eric Cornell, Wolfgang Ketterle and Steve Girvin.

APPENDIX A

In this appendix we go through some of the technicalities of the calculation of the one-loop Feynman diagrams for the coupling constants Γ_{11} and Γ_{12} , i.e. essentially the normal and anomalous selfenergies, and explicitly show the Hugenholtz-Pines theorem to hold in our renormalization group approach. This theorem states that [35]

$$\mu = \hbar\Sigma_{11}(\mathbf{0}; 0) - \hbar\Sigma_{12}(\mathbf{0}; 0) , \tag{A.1}$$

where $\hbar\Sigma_{11}(\mathbf{0}; 0)$ and $\hbar\Sigma_{12}(\mathbf{0}; 0)$ are the irreducible normal and anomalous selfenergies respectively. In our notation this relation reads

$$\Gamma_{11} = \Gamma_{12} . \tag{A.2}$$

Fig. 7 in the main text contains the diagrams renormalizing Γ_{12} and in Fig. 12 we depict the one-loop diagrams renormalizing Γ_{11} . Using the designation of the diagrams as in these figures one can show, after going through the combinatorics, that the (infinitesimal) change of the vertices after integrating out an infinitesimal momentum shell is given by

$$d\Gamma_{11} = 4d\Gamma_{11}^A + 4d\Gamma_{11}^B + 2d\Gamma_{11}^C + 4d\Gamma_{11}^D + 4d\Gamma_{11}^E + 4d\Gamma_{11}^F + 4\Gamma_3 d(\sqrt{n_0}) , \quad (\text{A.3a})$$

$$d\Gamma_{12} = 2d\Gamma_{12}^A + 4d\Gamma_{12}^B + 4d\Gamma_{12}^C + 4d\Gamma_{12}^D + 4d\Gamma_{12}^E + 2d\Gamma_{12}^F + 2\Gamma_3 d(\sqrt{n_0}) . \quad (\text{A.3b})$$

The last term in both expressions originates from the shift in $a_{\mathbf{0},0}$ required to eliminate the linear term $d\Gamma_0(a_{\mathbf{0},0}^* + a_{\mathbf{0},0})$ from the action. From Figs. 7 and 12 it is clear that a number of diagrams contributing to Γ_{11} or Γ_{12} are mathematically identical. Most notably we have $d\Gamma_{11}^B = d\Gamma_{11}^F = d\Gamma_{12}^D = d\Gamma_{12}^E$, $d\Gamma_{11}^D = d\Gamma_{12}^C = d\Gamma_{12}^F$, and $d\Gamma_{11}^E = d\Gamma_{12}^B$. Therefore, there are only six independent diagrams, namely $d\Gamma_{11}^A, d\Gamma_{11}^B, d\Gamma_{11}^C, d\Gamma_{11}^D, d\Gamma_{11}^E$, and $d\Gamma_{12}^A$. Using the Bogoliubov transformation from Eq. (35), it follows that

$$\langle a_{\mathbf{k},n}^* a_{\mathbf{k},n} \rangle = u_{\mathbf{k}}^2 \langle b_{\mathbf{k},n}^* b_{\mathbf{k},n} \rangle + v_{\mathbf{k}}^2 \langle b_{-\mathbf{k},-n}^* b_{-\mathbf{k},-n} \rangle , \quad (\text{A.4})$$

$$\langle a_{\mathbf{k},n}^* a_{-\mathbf{k},-n}^* \rangle = \langle a_{\mathbf{k},n} a_{-\mathbf{k},-n} \rangle = -u_{\mathbf{k}} v_{\mathbf{k}} (\langle b_{\mathbf{k},n}^* b_{\mathbf{k},n} \rangle + \langle b_{-\mathbf{k},-n}^* b_{-\mathbf{k},-n} \rangle) , \quad (\text{A.5})$$

with $u_{\mathbf{k}}$ and $v_{\mathbf{k}}$ given in Eq. (36), and these diagrams are now straightforward to calculate by applying the usual Feynman rules [34]. We have

$$d\Gamma_{11}^A = \frac{1}{2} V_0 dn' = \frac{\Lambda^3}{4\pi^2} V_0 \left(\frac{1}{2} (u_{\Lambda}^2 + v_{\Lambda}^2) (2N(\hbar\omega_{\Lambda}) + 1) - \frac{1}{2} \right) e^{-3l} dl , \quad (\text{A.6a})$$

$$d\Gamma_{11}^B = \frac{\Lambda^3}{2\pi^2} \Gamma_3^2 (u_{\Lambda}^3 v_{\Lambda} + u_{\Lambda} v_{\Lambda}^3) \left(\frac{1 + 2N(\hbar\omega_{\Lambda})}{2\hbar\omega_{\Lambda}} + \beta N(\hbar\omega_{\Lambda}) [N(\hbar\omega_{\Lambda}) + 1] \right) e^{-3l} dl , \quad (\text{A.6b})$$

$$d\Gamma_{11}^C = -\frac{\Lambda^3}{2\pi^2} \Gamma_3^2 \left((u_{\Lambda}^4 + v_{\Lambda}^4) \frac{1 + 2N(\hbar\omega_{\Lambda})}{2\hbar\omega_{\Lambda}} + 2u_{\Lambda}^2 v_{\Lambda}^2 \beta N(\hbar\omega_{\Lambda}) [N(\hbar\omega_{\Lambda}) + 1] \right) e^{-3l} dl , \quad (\text{A.6c})$$

$$d\Gamma_{11}^D = -\frac{\Lambda^3}{\pi^2} \Gamma_3^2 u_\Lambda^2 v_\Lambda^2 \left(\frac{1 + 2N(\hbar\omega_\Lambda)}{2\hbar\omega_\Lambda} + \beta N(\hbar\omega_\Lambda)[N(\hbar\omega_\Lambda) + 1] \right) e^{-3l} dl, \quad (\text{A.6d})$$

$$d\Gamma_{11}^E = -\frac{\Lambda^3}{2\pi^2} \Gamma_3^2 \left(2u_\Lambda^2 v_\Lambda^2 \frac{1 + 2N(\hbar\omega_\Lambda)}{2\hbar\omega_\Lambda} + (u_\Lambda^4 + v_\Lambda^4) \beta N(\hbar\omega_\Lambda)[N(\hbar\omega_\Lambda) + 1] \right) e^{-3l} dl, \quad (\text{A.6e})$$

$$d\Gamma_{12}^A = \frac{1}{2} V_{\mathbf{0}} d\tilde{n} = -\frac{\Lambda^3}{4\pi^2} V_{\mathbf{0}} u_\Lambda v_\Lambda (1 + 2N(\hbar\omega_\Lambda)) e^{-3l} dl, \quad (\text{A.6f})$$

introducing $dn' = \Lambda^3 \sum_n \langle a_{\Lambda,n}^* a_{\Lambda,n} \rangle e^{-3l} dl / 2\pi^2$ and $d\tilde{n} = \Lambda^3 \sum_n \langle a_{\Lambda,n}^* a_{-\Lambda,-n}^* \rangle e^{-3l} dl / 2\pi^2$ with which one can easily verify that

$$d(\sqrt{n_{\mathbf{0}}}) = -\frac{d\Gamma_{\mathbf{0}}}{\Gamma_{11} + \Gamma_{12}} = -\frac{1}{\Gamma_{11} + \Gamma_{12}} \Gamma_3 (2dn' + d\tilde{n}). \quad (\text{A.7})$$

Combining these equations leads to the flow equations for Γ_{11} and Γ_{12} . However, we here concentrate on the Hugenholtz-Pines relation, which is satisfied at $l = 0$, and therefore remains valid if also $d\Gamma_{11} = d\Gamma_{12}$ at $l = 0$. Using the above mentioned equalities of the various diagrams, this equality reduces in first instance to

$$2d\Gamma_{11}^A + d\Gamma_{11}^C + \Gamma_3 d(\sqrt{n_{\mathbf{0}}}) = d\Gamma_{12}^A + d\Gamma_{12}^C = d\Gamma_{12}^A + d\Gamma_{11}^D. \quad (\text{A.8})$$

However, due to the $U(1)$ -symmetry of the action $S[\psi^*, \psi]$ we have at any value of l that $\Gamma_3^2 = n_{\mathbf{0}} V_{\mathbf{0}}^2 = \Gamma_{12} V_{\mathbf{0}}$ and at $l = 0$, when $\Gamma_{11} = \Gamma_{12}$, Eq. (A.8) reduces with the help of Eq. (A.7) to

$$d\Gamma_{11}^C - d\Gamma_{11}^D = V_{\mathbf{0}} d\tilde{n}, \quad (\text{A.9})$$

or equivalently

$$-\frac{\Lambda^3}{2\pi^2} \Gamma_3^2 (u_\Lambda^4 - 2u_\Lambda^2 v_\Lambda^2 + v_\Lambda^4) \frac{1 + 2N(\hbar\omega_\Lambda)}{2\hbar\omega_\Lambda} = -\frac{\Lambda^3}{2\pi^2} V_{\mathbf{0}} u_\Lambda v_\Lambda (1 + 2N(\hbar\omega_\Lambda)). \quad (\text{A.10})$$

Note that, due to the fact that $u_\Lambda^2 - v_\Lambda^2 = 1$, the left-hand side of this equation actually does not contain Bogoliubov coherence factors. From the definition of the coherence factors in Eq.

(36) it is now easy to show that indeed, at $l = 0$, we have $d\Gamma_{11} = d\Gamma_{12}$ and as a consequence that the Hugenholtz-Pines relation remains valid at any point during the integration.

Next, we briefly turn to the regime $na\Lambda_{th}^2 \ll 1$ where we put $u_{\mathbf{k}} = 1$ and $v_{\mathbf{k}} = 0$ in contributions containing infrared divergencies. In this case, only the first term in the left-hand side of Eq. (A.10) contributes, but now with a factor 1 instead of u_{Λ}^4 . Thus, nothing changes with respect to the previous situation, and the Hugenholtz-Pines relation is again valid at any point during the renormalization if we still use the exact expressions for $u_{\mathbf{k}}$ and $v_{\mathbf{k}}$ in contributions not containing infrared divergencies, and most importantly in $d\tilde{n}$.

APPENDIX B

In this appendix we discuss the implications of anomalous scaling, focussing on the situation at the critical temperature where the coupling constants flow into the fixed point $(\mu^*, V_{\mathbf{0}}^*)$. We start with the fundamental statement from renormalization group theory that the exact n -point vertex function remains identical during renormalization, i.e. in our case

$$\Gamma^{(n)}(p_i, \omega_i; \mu, V_{\mathbf{0}}, T; \Lambda) = \Gamma^{(n)}(p_i, \omega_i; \mu(l), V_{\mathbf{0}}(l), T(l); \Lambda e^{-l}), \quad (\text{B.1})$$

where $p_i < \Lambda e^{-l}$. The coupling constants obey the derived renormalization group equations (without trivial scaling) and $T(l) = T e^{2l}$. When we are at the critical temperature, we can take $\omega_i = 0$ and we find after performing the trivial rescaling that

$$\Gamma^{(n)}(p_i, 0; \mu, V_{\mathbf{0}}, T_c; \Lambda) = e^{-(3-\frac{n}{2})l} \Gamma^{(n)}(p_i e^l, 0; \mu(l), V_{\mathbf{0}}(l), T_c(l); \Lambda). \quad (\text{B.2})$$

A dimensional analysis then shows that

$$\Gamma^{(n)}(p_i e^l, 0; \mu(l), V_{\mathbf{0}}(l), T_c(l); \Lambda) = \Lambda^{3-\frac{n}{2}} \Gamma^{(n)}\left(\frac{p_i e^l}{\Lambda}, 0; \frac{\mu(l)}{\Lambda^2}, \frac{V_{\mathbf{0}}(l)}{\Lambda}, \frac{T_c(l)}{\Lambda^2}; 1\right). \quad (\text{B.3})$$

Combining these two equations, and taking the limit $l \rightarrow \infty$ in which we approach the fixed point, this implies

$$\Gamma^{(n)}(p_i, 0; \mu, V_{\mathbf{0}}, T_c; \Lambda) = \Lambda^{3-\frac{n}{2}}(l) \Gamma^{(n)}\left(\frac{p_i}{\Lambda(l)}, 0; \frac{\mu^*}{\Lambda^2}, \frac{V_{\mathbf{0}}^*}{\Lambda}, \infty; 1\right) \equiv \Lambda^{3-\frac{n}{2}}(l) \Gamma^{(n)*}\left(\frac{p_i}{\Lambda(l)}\right). \quad (\text{B.4})$$

The right-hand side has, just like the left-hand side, to be independent of l , and this leads to the conclusion that

$$\Gamma^{(n)*}\left(\frac{p_i}{\Lambda(l)}\right) = \Lambda^{\frac{n}{2}-3}(l)\Gamma^{(n)*}(p_i) \quad (\text{B.5})$$

or that $\Gamma^{(n)*}(p_i)$ has to be a homogeneous function of degree $(3 - n/2)$. Thus

$$\Gamma^{(n)*}(\lambda p_i) = \lambda^{3-\frac{n}{2}}\Gamma^{(n)*}(p_i) \quad (\text{B.6})$$

and we can conclude that anomalous scaling reveals information about the momentum dependence of the n -point vertex function. In particular, we have e.g. for the selfenergy at the critical temperature that

$$\Gamma^{(2)*}(k) \propto k^2, \quad (\text{B.7})$$

and most importantly for the four-point function that

$$\Gamma^{(4)*}(\mathbf{k}, \mathbf{k}', \mathbf{K}) \propto (|\mathbf{k}| + |\mathbf{k}'|) + \alpha |\mathbf{K}|, \quad (\text{B.8})$$

which shows that the effective interaction at long wavelengths has to vanish at the critical temperature.

Clearly, the above reasoning is in principle not restricted to the critical temperature and a similar argument can be set up also for arbitrary temperatures. As a result, the anomalous scaling we find from the set of renormalization group equations derived in Sec. IVA for the symmetry broken phase also implies a nontrivial momentum dependence of the coupling constants.

REFERENCES

- [1] M.H. Anderson, J.R. Ensher, M.R. Matthews, C.E. Wieman and E.A. Cornell, *Science* **269**, 198 (1995).
- [2] K.B. Davis, M.O. Mewes, M.R. Andrews, N.J. van Druten, D.S. Durfee, D.M. Kurn and W. Ketterle, *Phys. Rev. Lett.* **75**, 3969 (1995).
- [3] C.C. Bradley, C.A. Sackett, J.J. Tollett and R.G. Hulet, *Phys. Rev. Lett.* **75**, 1687 (1995).
- [4] H.T.C. Stoof, *Phys. Rev. A* **49**, 3824 (1994).
- [5] P.A. Ruprecht, M.J. Holland, K. Burnett, and M. Edwards, *Phys. Rev. A* **51**, 4704 (1995).
- [6] H.T.C. Stoof, (unpublished, cond-mat/9601150).
- [7] S. Stringari, *Phys. Rev. Lett.* **76**, 1405 (1996).
- [8] H.T.C. Stoof, *Phys. Rev. Lett.* **66**, 3148 (1991); *Phys. Rev. A* **45**, 8398 (1992).
- [9] F. Dalfovo, L. Pitaevskii, S. Stringari, (unpublished, cond-mat/9604069).
- [10] M. Edwards and K. Burnett, *Phys. Rev. A* **51**, 1382 (1995).
- [11] S. Stringari, (unpublished, cond-mat/9603126).
- [12] A.L. Fetter, *Phys. Rev. A* **53**, 4245 (1996).
- [13] M. Edwards, P.A. Ruprecht, K. Burnett, R.J. Dodd and C.W. Clark, (unpublished, cond-mat/9605170).
- [14] H.T.C. Stoof, M. Houbiers, C.A. Sackett and R.G. Hulet, *Phys. Rev. Lett.* **76**, 10 (1996).
- [15] M. Bijlsma and H.T.C. Stoof, (unpublished, cond-mat/9507134).
- [16] A. Griffin, *Physica C* **156**, 12 (1988).

- [17] H. Shi, G. Verechaka and A. Griffin, *Phys. Rev. B* **50**, 1119 (1994).
- [18] T.D. Lee and C.N. Yang, *Phys. Rev.* **112**, 1419 (1958).
- [19] L. Reatto and J.P. Straley, *Phys. Rev.* **183**, 321 (1969).
- [20] M. Bijlsma and H.T.C. Stoof, (unpublished, cond-mat/9605120).
- [21] K.G. Wilson and J. Kogut, *Phys. Rep.* **12**, 75 (1974).
- [22] D.S. Fisher and P.C. Hohenberg, *Phys. Rev. B* **37**, 4936 (1988).
- [23] P.B. Weichmann, *Phys. Rev. B* **38**, 8739 (1988).
- [24] E.B. Kolomeisky and J.P. Straley, *Phys. Rev. B* **46**, 11749 (1992).
- [25] E.B. Kolomeisky and J.P. Straley, *Phys. Rev. B* **46**, 13942 (1992).
- [26] E. Tiesinga, C.J. Williams, P.S. Julienne, K.M. Jones, P.D. Lett and W.D. Phillips, (unpublished).
- [27] See for example J.W. Negele and H. Orland, *Quantum Many-Particle Systems* (Addison-Wesley, New York, 1988).
- [28] R. Shankar, *Rev. Mod. Phys.* **66**, 129 (1994).
- [29] W. Glöckle, *The Quantum Mechanical Few-Body Problem* (Springer, Berlin, 1983).
- [30] K. Halpern and K. Huang, *Phys. Rev. Lett.* **74**, 3526 (1995).
- [31] J. Zinn-Justin, *Quantum Field Theory and Critical Phenomena* (Oxford University Press Inc., New York, 1989).
- [32] H.T.C. Stoof, M. Bijlsma and M. Houbiers, (accepted for publication in the NIST Journal of Physics).
- [33] V.N. Popov, *Functional Integrals in Quantum Field Theory and Statistical Physics* (Reidel, Dordrecht, 1983), Chap. 6.

- [34] A.L. Fetter and J.D. Walecka, *Quantum Theory of Many-Particle Systems* (McGraw-Hill, New York, 1971), Chapter 10.
- [35] N.M. Hugenholtz and D. Pines, Phys. Rev. **116**, 489 (1958).
- [36] P. Grüter, D. Ceperley, M. Dewing and F. Laloë, (private communication).
- [37] S. Giorgini, L.P. Pitaevskii and S. Stringari, (unpublished, cond-mat/9607117).
- [38] A. Griffin, *Excitations in a Bose-Condensed Liquid*, (Cambridge University Press, New York, 1993).
- [39] Yu. A. Nepomnyashchiĭ and A.A. Nepomnyashchiĭ, Zh. Eksp. Teor. Fiz. **75**, 976 (1978), [Sov. Phys. JETP **48**, 493 (1979)].

FIGURE CAPTIONS

Fig. 1 Typical behavior of the Fourier transform of the interatomic interaction potential $V(\mathbf{x} - \mathbf{x}')$.

Fig. 2 The one-loop Feynman graphs contributing to the renormalization of (a) the chemical potential, (b) the two-body interaction, and (c) the three-body interaction. The dot represents the two-body vertex V_0 and the square the three-body vertex U_0 .

Fig. 3 The $p - n^{-1}$ -diagram including (solid line) and excluding (dashed line) a three-body interaction term for atomic ^{23}Na at a temperature of $0.1\mu\text{K}$. The influence of U_0 is approximately 1.5 % near the critical density.

Fig. 4 The ratio of the many-body scattering lengths a^{RG} including (solid line) and excluding (dashed line) the bubble diagrams in the flow equations as a function of T/T_c for atomic ^{23}Na at a density of $1.5 \cdot 10^{12} \text{ cm}^{-3}$.

Fig. 5 Flow diagram resulting from the renormalization group equations. The fixed point is indicated with an asterisk.

Fig. 6 The critical degeneracy parameter $n_c \Lambda_{th}^3$ found from the renormalization group calculation as a function of a/Λ_{th} .

Fig. 7 The one-loop Feynman diagrams contributing to the renormalization of (a) the linear term and (b) the anomalous selfenergy in the broken phase. The filled circle represents the vertex V_0 and the open circle the vertex Γ_3 .

Fig. 8 The ratio of the effective scattering length a^{eff} and the two-body scattering length

a for atomic ^{23}Na at a density of $1.5 \cdot 10^{12} \text{ cm}^{-3}$. The dashed line corresponds to the result from the many-body T -matrix calculation, i.e. $a^{eff} = a^{MB}$. The solid lines correspond to the result from the renormalization group approach, i.e. $a^{eff} = a^{RG}$, with bubble diagrams included and excluded. The effect of the bubbles (lower solid line) is seen to be considerable, certainly below the critical temperature.

Fig. 9 The degeneracy parameter $n\Lambda_{th}^3$ as a function of the fugacity ζ for the ideal gas (dotted line), from the many-body T -matrix theory (dashed line) and as found from the renormalization group calculation (solid line).

Fig. 10 (a) The condensate fraction and (b) the superfluid fraction as a function of temperature for a density of $1.5 \cdot 10^{12}$ sodium atoms per cubic centimeter, both from the many-body T -matrix calculation (dashed line) as from the renormalization group calculation (solid line).

Fig. 11 The pressure as a function of inverse density for atomic ^{23}Na at a temperature of $0.1\mu\text{K}$. The dashed line is the result from the many-body T -matrix calculation, the solid line from the renormalization group calculation.

Fig. 12 The one-loop Feynman diagrams contributing to the renormalization of the normal selfenergy in the broken phase. The filled circle represents the vertex V_0 and the open circle the vertex Γ_3 .

Fig. 1 Bijlsma et. al.

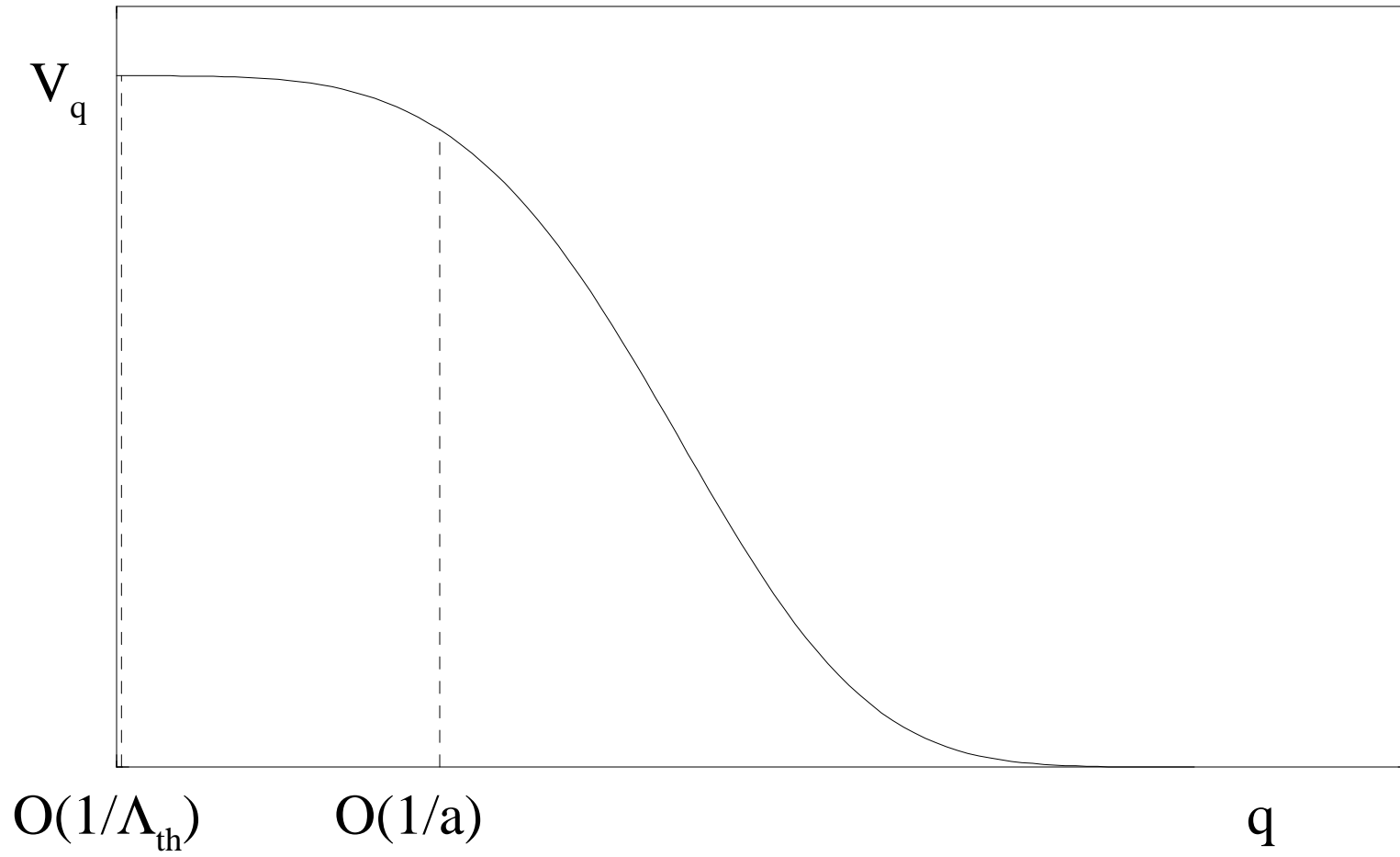


Fig. 2 Bijlsma et. al.

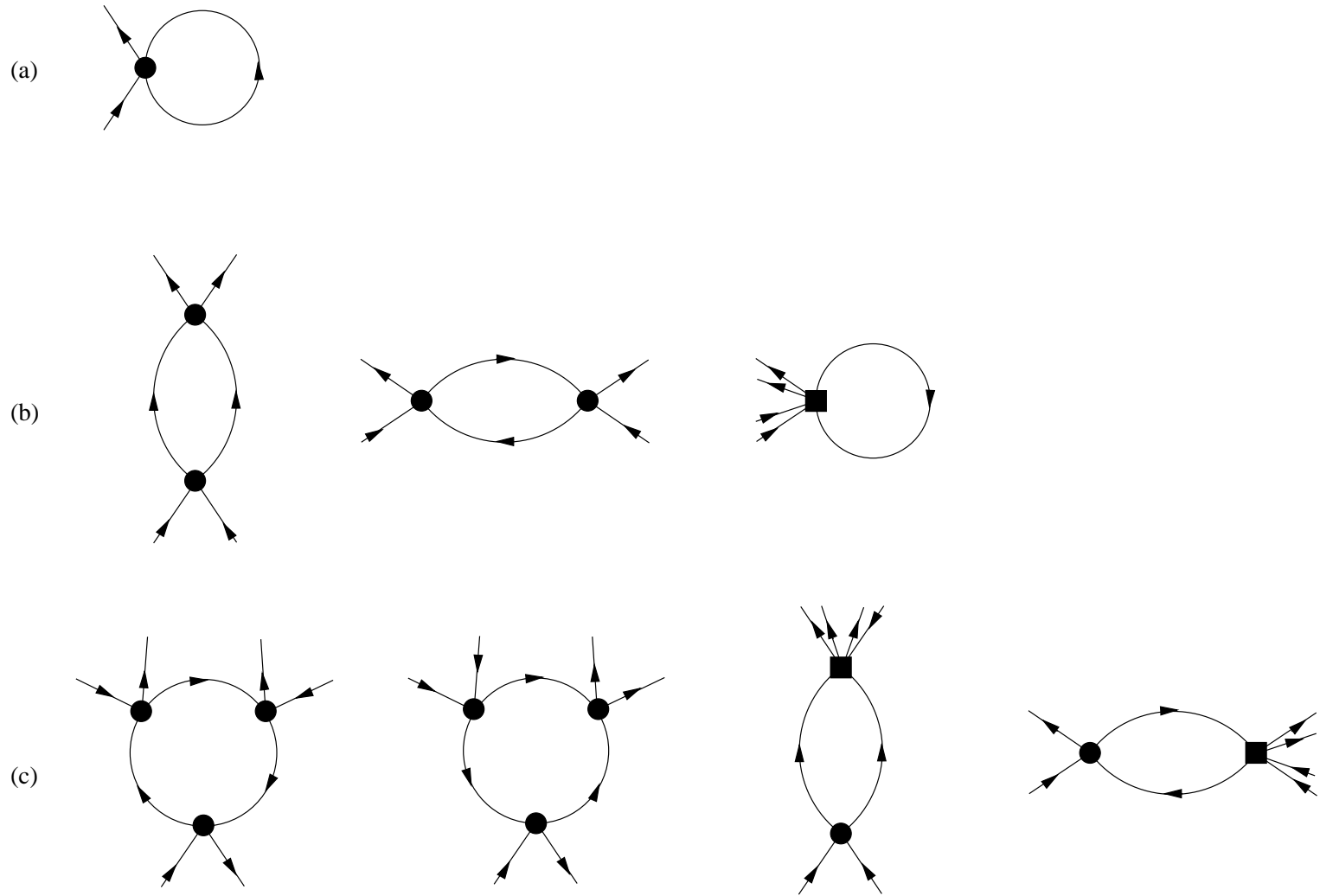


Fig. 3 Bijlsma et. al.

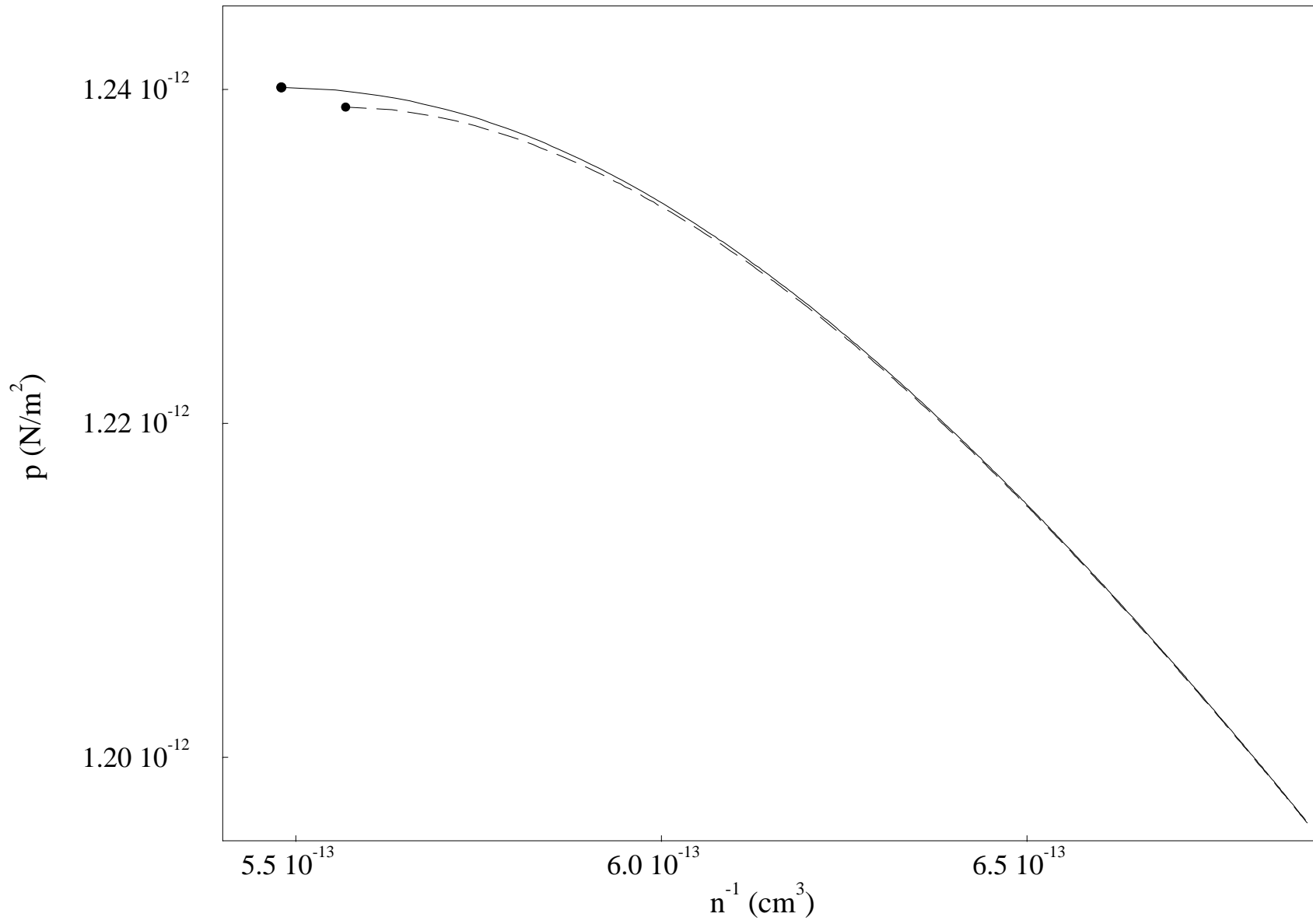


Fig. 4 Bijlsma et. al.

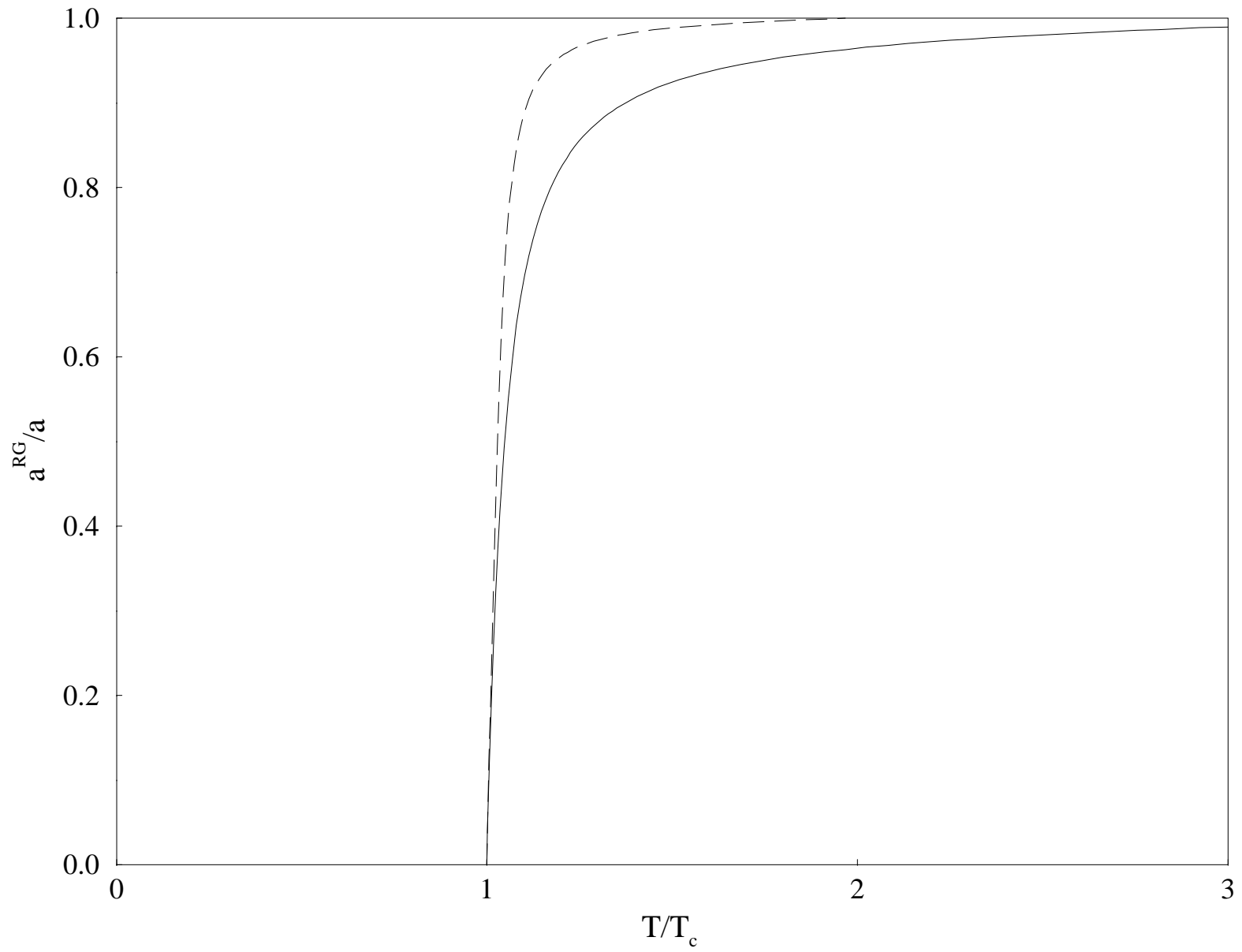


Fig. 5 Bijlsma et. al.

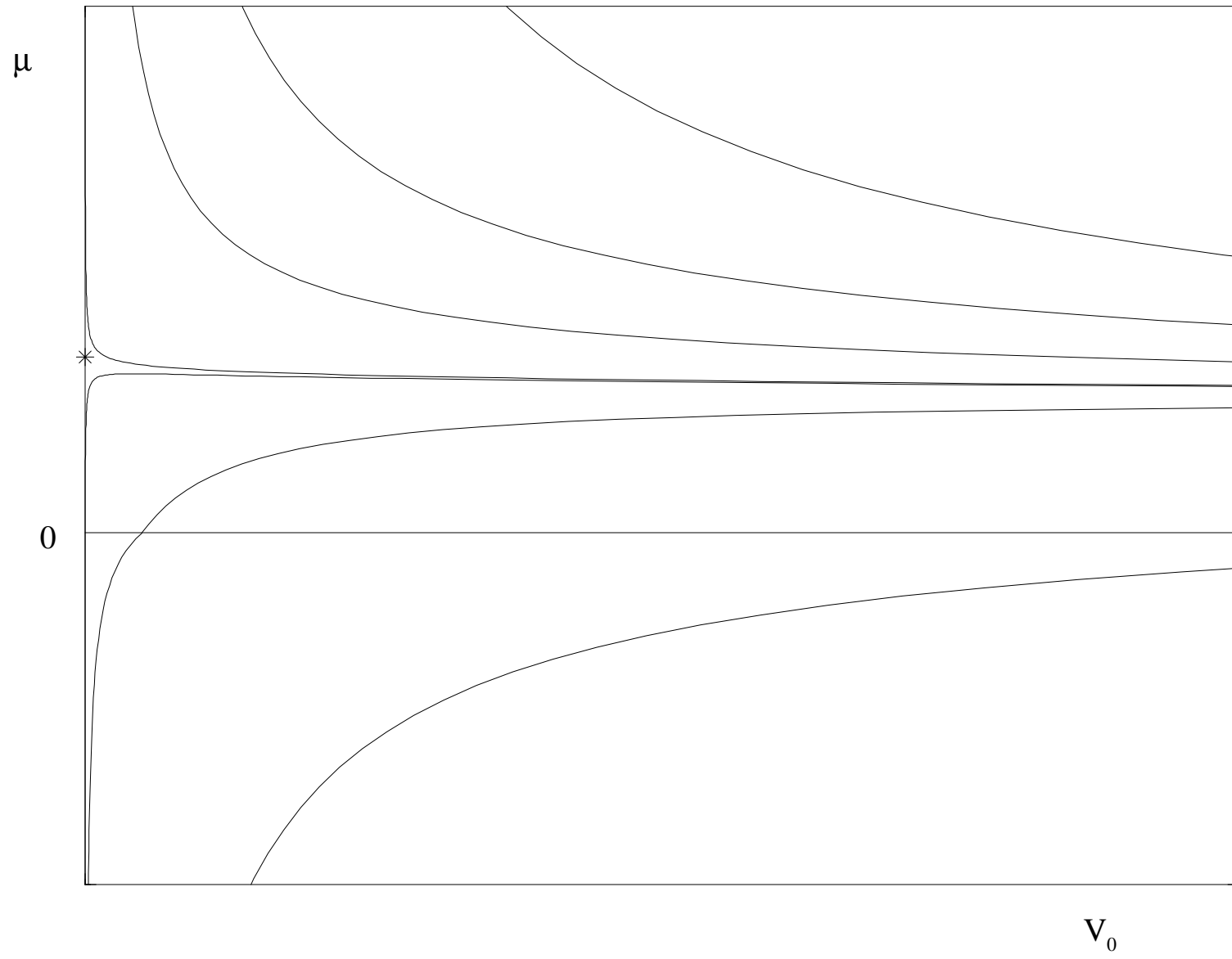


Fig. 6 Bijlsma et. al.

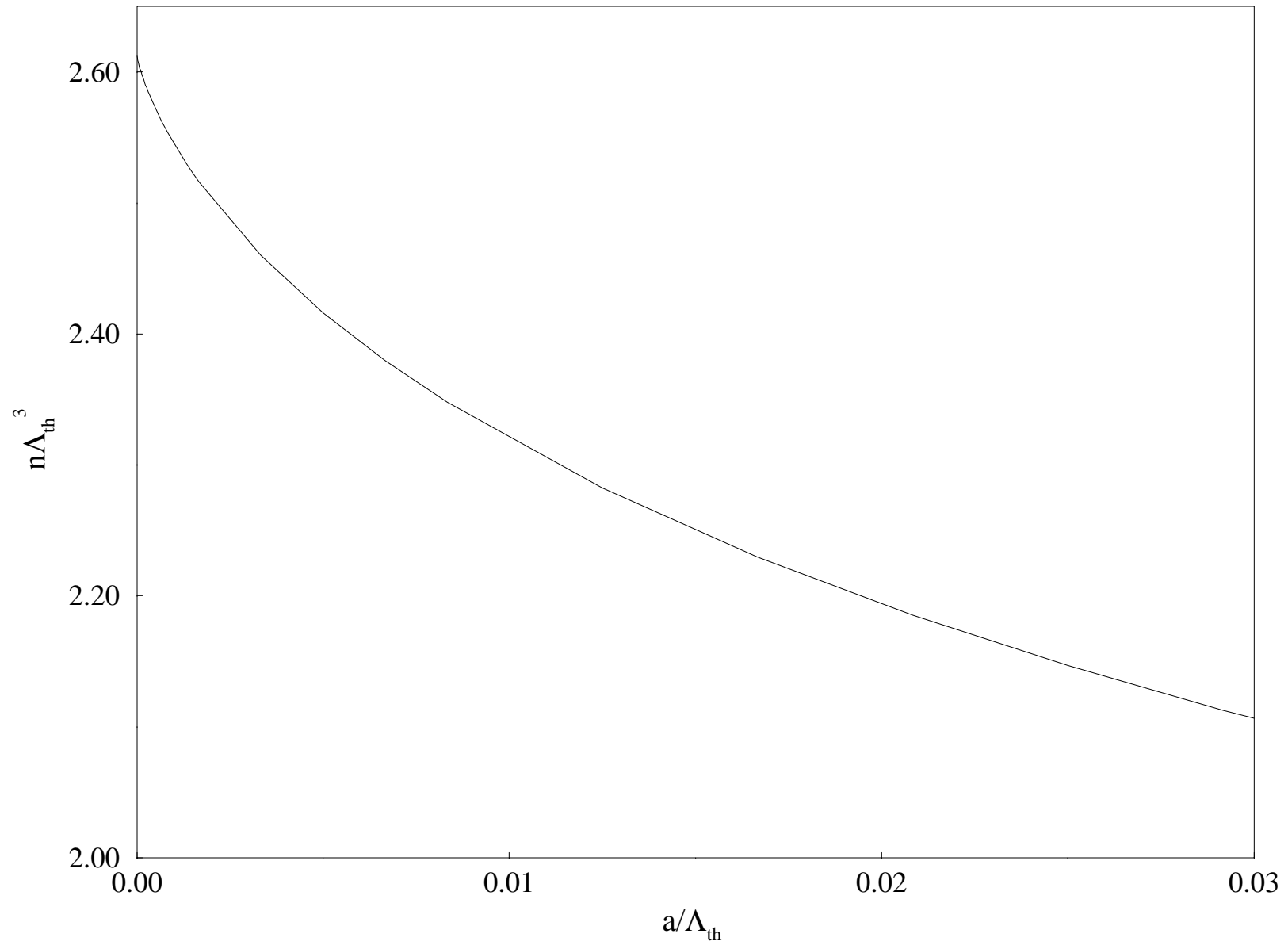


Fig. 7 Bijlsma et. al.

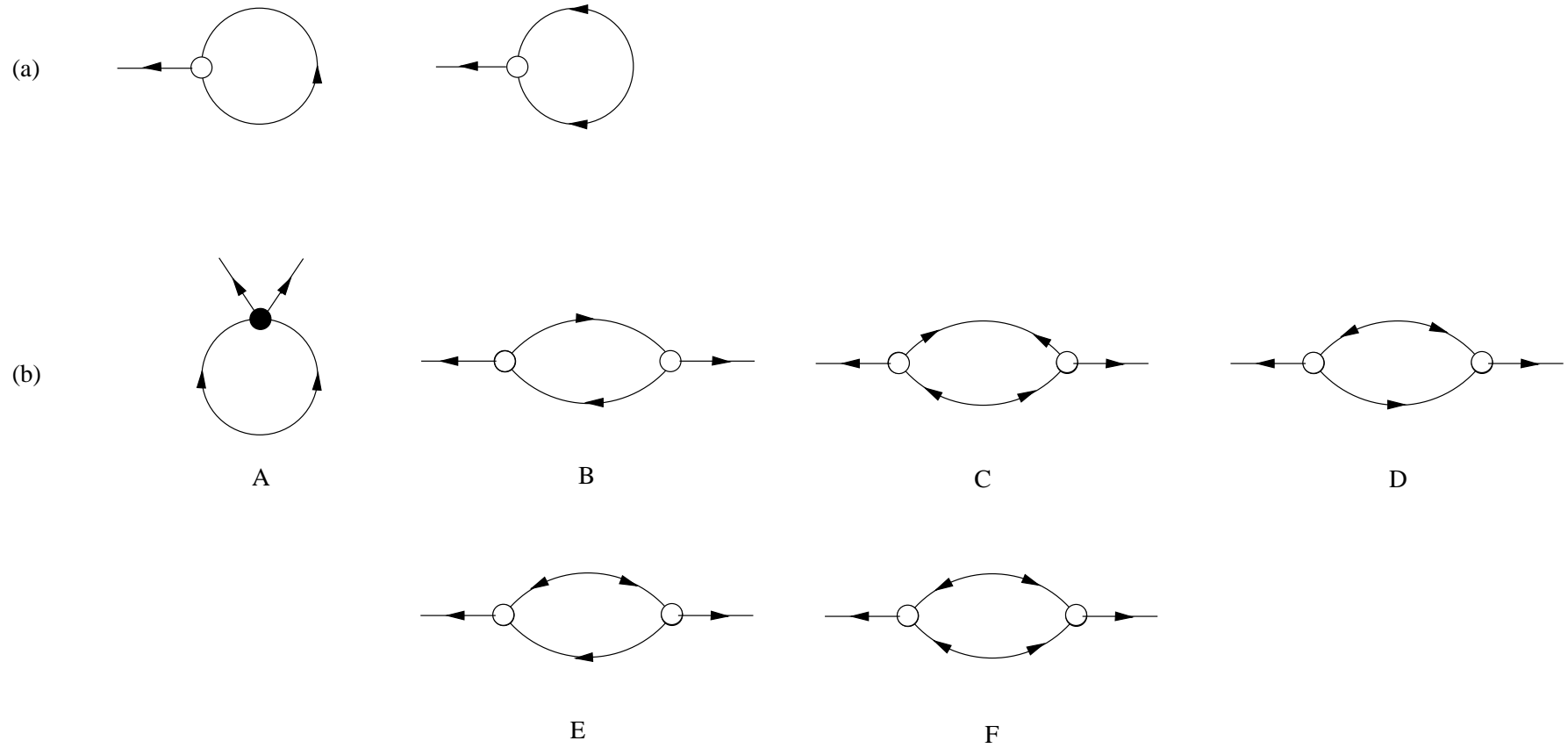


Fig. 8 Bijlsma et. al.

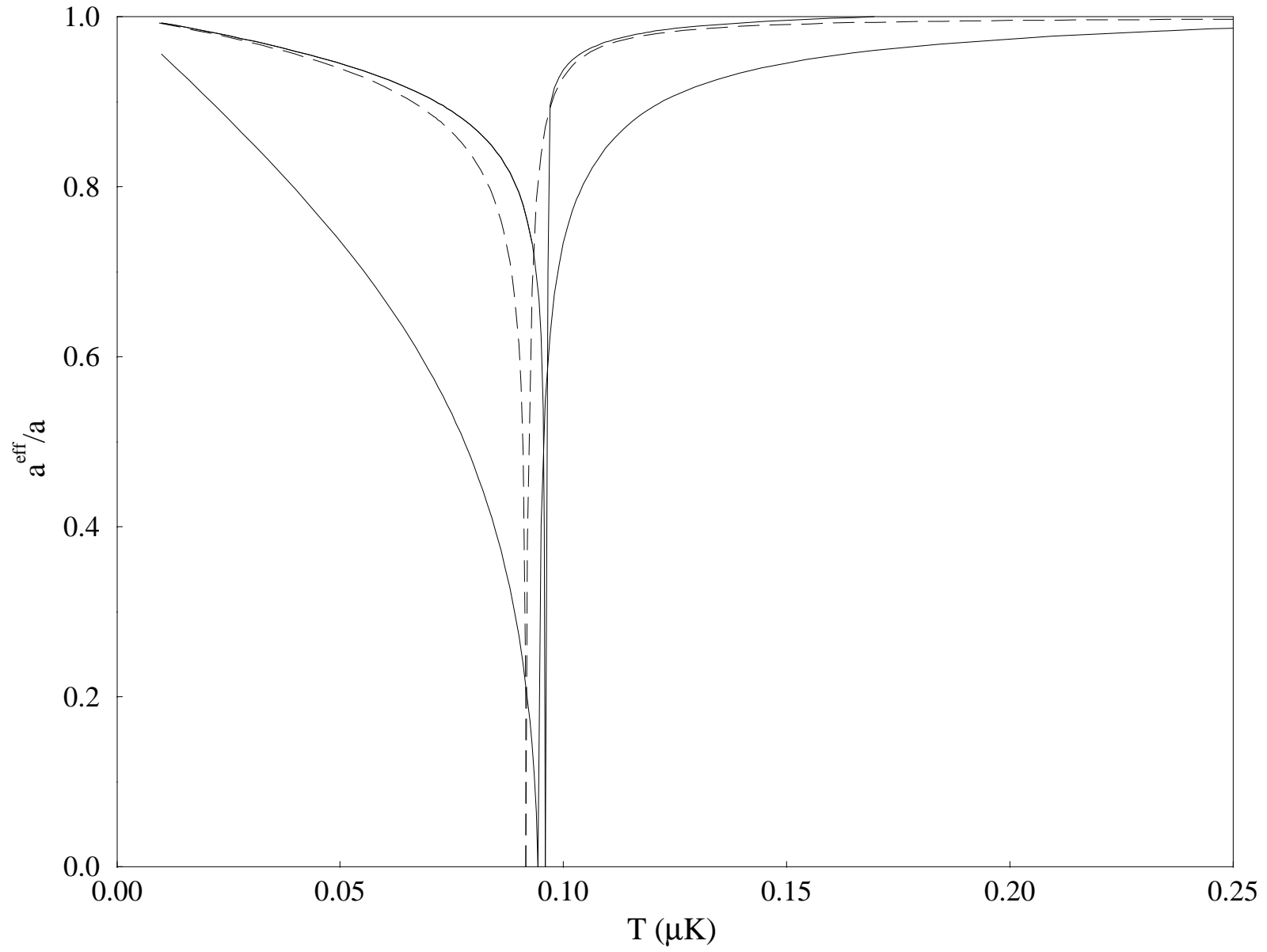


Fig. 9 Bijlsma et. al.

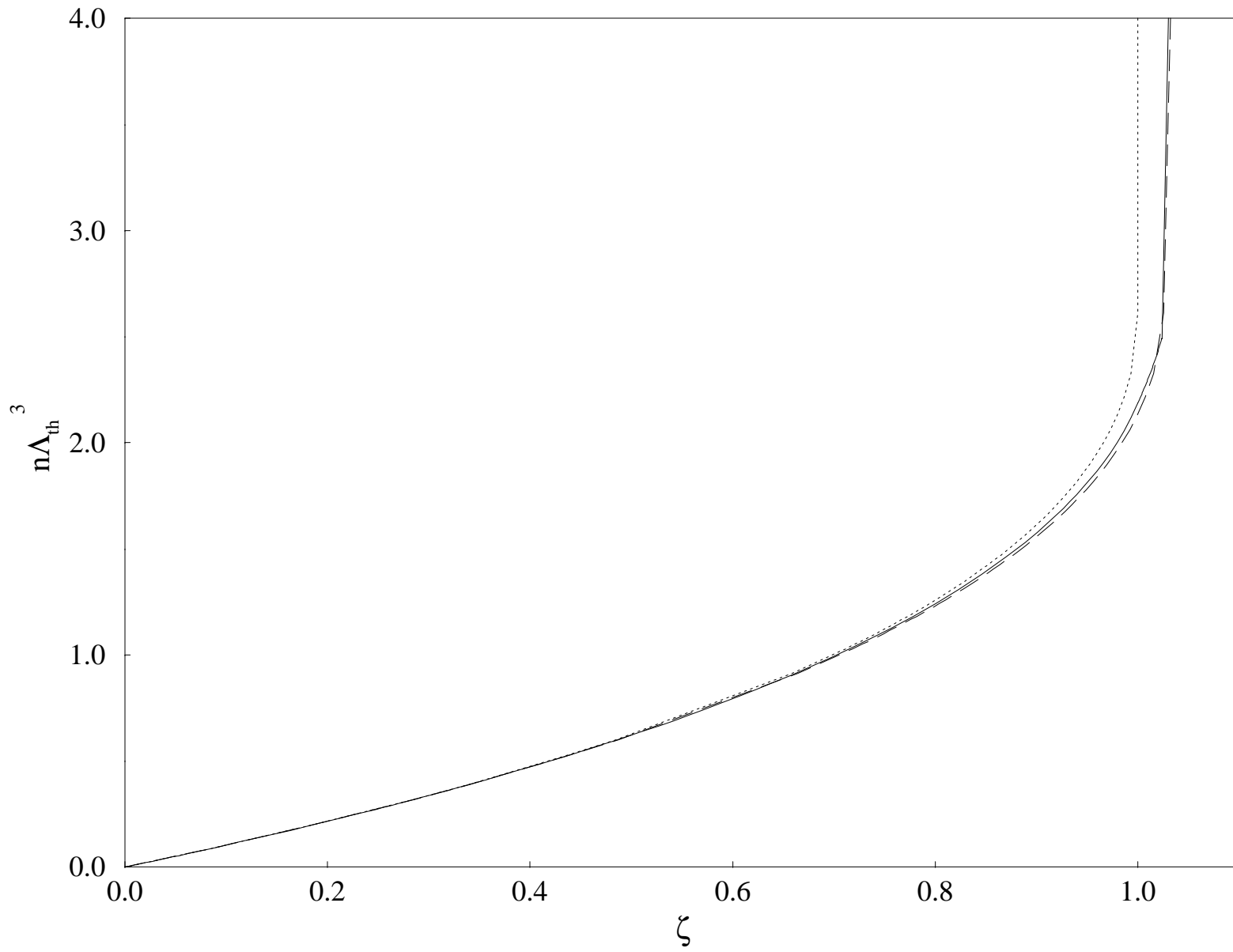


Fig. 10(a) Bijlsma et. al.

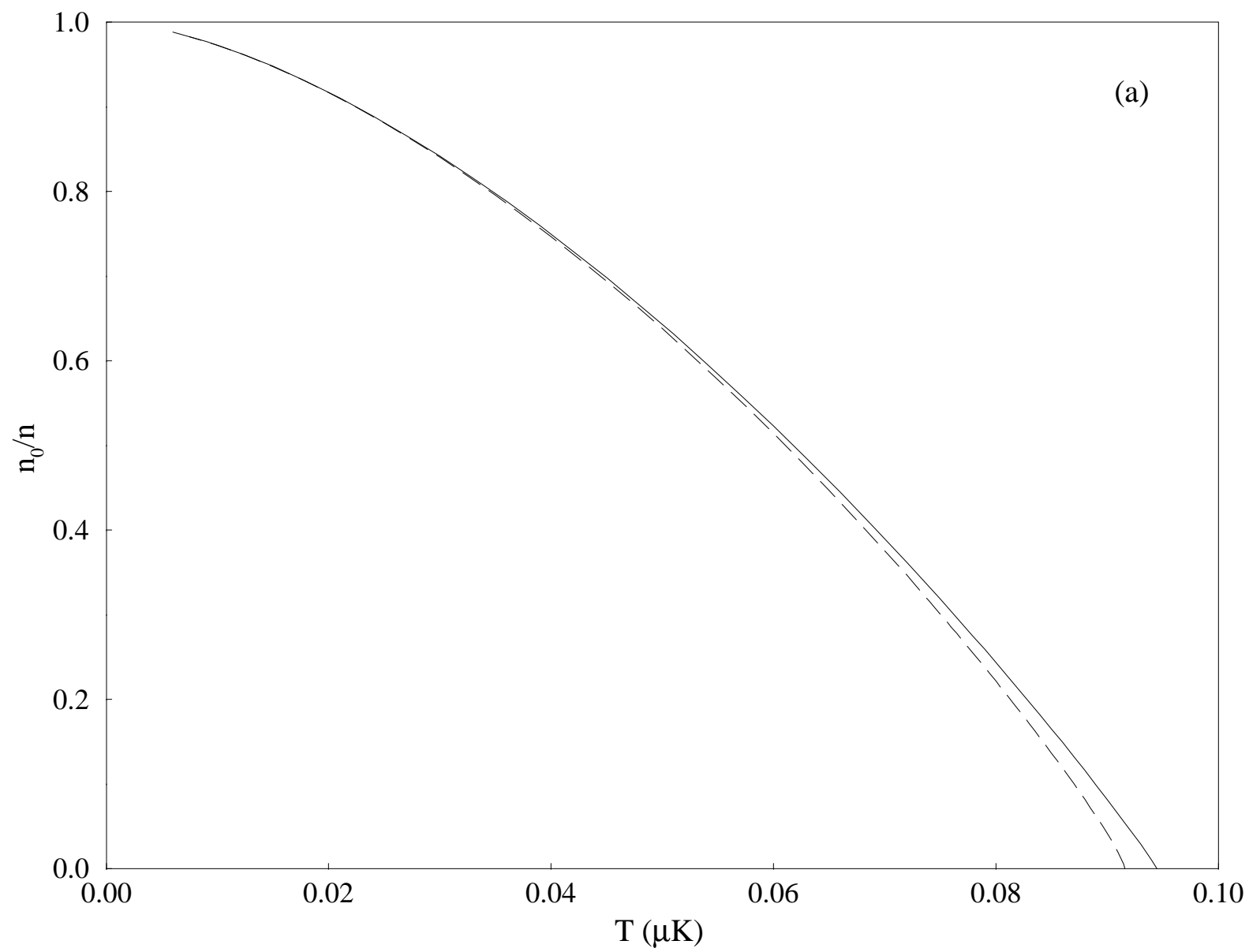


Fig. 10(b) Bijlsma et. al.

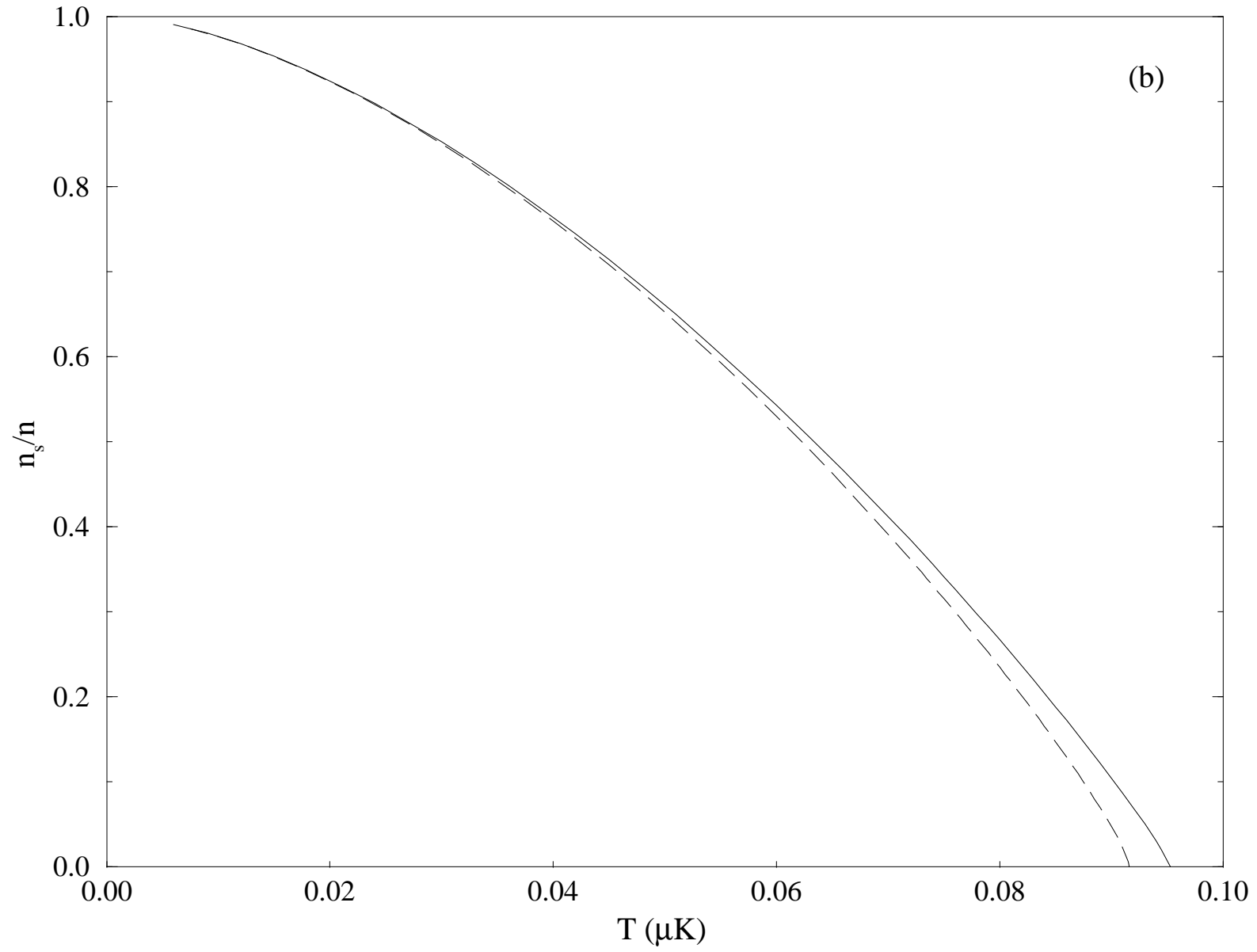


Fig. 11 Bijlsma et. al.

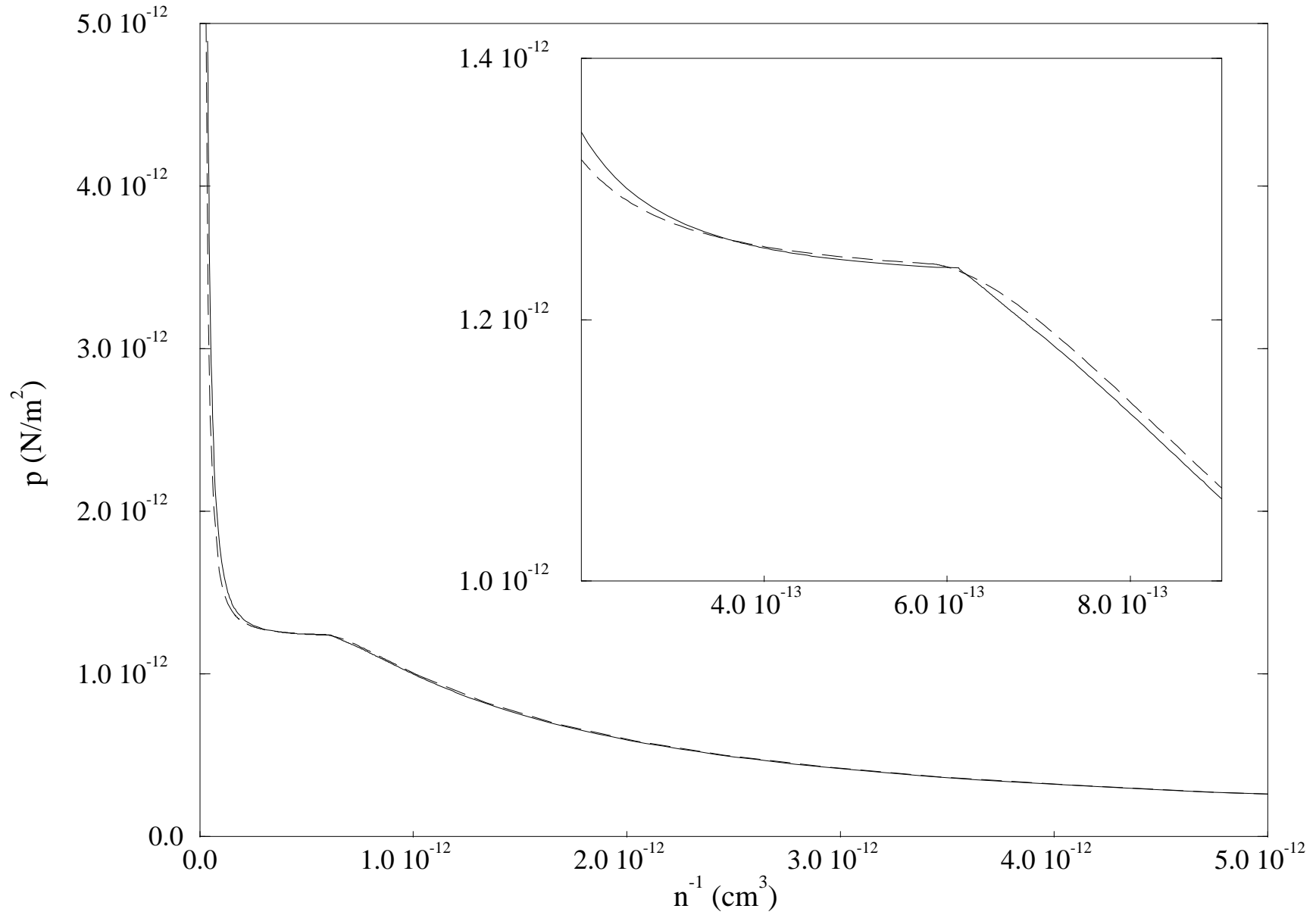
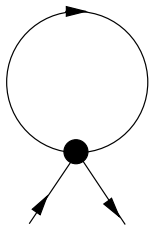
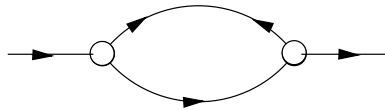


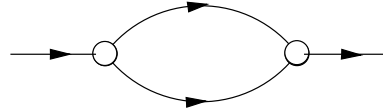
Fig. 12 Bijlsma et. al.



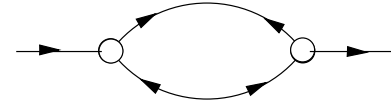
A



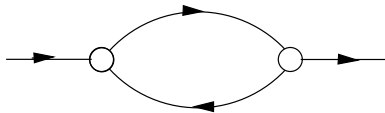
B



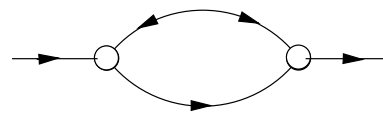
C



D



E



F